Plant Biotechnology Journal
Open Access

Plant Biotechnology Journal (2025) **23**, pp. 1909–1926 doi: 10.1111/pbi.70020

Gibberellin signalling mediates nucleocytoplasmic trafficking of Sucrose Synthase 1 to regulate the drought tolerance in rice

Jishuai Huang[1,2], Bin Xie[1], Fengjun Xian[1], Kejia Liu[1], Qian Yan[1], Yurong He[1], Lin Zhu[1], Wei Liu[1], Yue Jiang[1], Yuting Chen[1], Leilei Peng[1], Yuwei Zhou[1] and Jun Hu[1,2,*]

[1]*State Key Laboratory of Hybrid Rice, College of Life Sciences, Wuhan University, Wuhan, China*
[2]*Engineering Research Center for Plant Biotechnology and Germplasm Utilization of Ministry of Education, College of Life Sciences, Wuhan University, Wuhan, China*

Received 22 October 2024;
revised 23 January 2025;
accepted 6 February 2025.
**Correspondence* (Tel +86 013707149400; fax +86 027-68752095; email junhu@whu.edu.cn)

Keywords: GA, sucrose, translocation, drought, crops.

Summary

The Green Revolution (GR) has substantially improved cereal crop yields and enhanced adaptation to diverse environmental challenges. However, the molecular and cellular mechanisms involving GR-related genes that regulate drought tolerance in plants remain largely unclear. Here, we reveal that the gibberellin (GA) signalling repressor SLENDER RICE 1 (SLR1) negatively regulates the abundance of the dehydration-responsive protein OsBURP3 to enhance drought tolerance in rice. OsBURP3 facilitates the translocation of Sucrose Synthase 1 (OsSUS1), from the cytosol to the nucleus, thereby decreasing the sucrose content. Mutation of *OsBURP3* reduces the nucleus accumulation of OsSUS1 to enhance drought tolerance. SLR1 also competitively associates with OsBURP3 in the nucleus to release OsSUS1 back into the cytosol, resulting in elevated sucrose content. Cytological evidences confirm that sucrose contributes to the fine-tuning of the stomata aperture in rice leaves. Collectively, these findings provide a comprehensive framework for understanding the role of GA in regulating drought tolerance by mediating sucrose metabolism in crops.

Introduction

The global population has surged to 9.7 billion in <30 years, necessitating a 40% increase in crop production to meet the growing food demand (Anderson *et al.*, 2020). However, drought remains the most complex and destructive environmental factor limiting yearly crop production and there is an urgent need to breed drought-tolerance crops that require less water for growth (Ahmad *et al.*, 2022). Over the past 50 years, extensive studies have advanced our understanding of the physiological, biochemical and molecular genetic mechanisms underlying plant responses to drought stress, with numerous genes implicated in these responses being extensively characterized (Fernando *et al.*, 2021; Sinclair, 2011). However, the intricate mechanisms underlying plant drought tolerance remain largely unexplored (Cominelli *et al.*, 2013; Cooper and Messina, 2023).

As sessile organisms, plants have developed intricate and highly sophisticated mechanisms to respond to environmental stress, enabling them to survive and achieve optimal yield under adverse conditions. Among these signals, plant hormones play a crucial role in these adaptive responses (Bari and Jones, 2009). In particular, dehydration triggers the accumulation of abscisic acid (ABA) in the leaf mesophyll cells, which subsequently activates downstream signalling pathways (Kalladan *et al.*, 2017; Tang *et al.*, 2016). ABA exerts its effects, in part, by inhibiting the brassinosteroid (BR) signalling pathway through activating the BR signalling negative regulator, BRASSINOSTEROID-INSENSITIVE 2 (BIN2), thereby contributing to drought resistance (Wang *et al.*, 2018). Additionally, the rice auxin-inducible gene *DEEPER ROOTING1* (DRO1) enhances drought tolerance by promoting the development of a more vertical and deeper root system architecture (Uga *et al.*, 2013). GAs also play a role in restricting plant growth under various stress conditions, including cold, salt, osmotic and drought stress (Colebrook *et al.*, 2014; Dubois *et al.*, 2013; Magome *et al.*, 2008). In rice, most GA metabolic genes are downregulated under water-deficit conditions, leading to reduced GA levels, inhibited growth and enhanced drought tolerance (Liao *et al.*, 2023).

The GR has increased cereal crop yields by strategically enhancing the harvest index, reducing plant height and increasing fertilizer use in crops such as wheat and rice (Liu *et al.*, 2021; Van De Velde *et al.*, 2017). High-yield semi-dwarf varieties were developed by mutations in the rice *semi-dwarf1* (*sd1*) gene, which encodes a GA biosynthetic enzyme, GA20-oxidase and in the wheat *Reduced height1* (*Rht1*) and *Rht2* genes, which encodes a DELLA protein. These mutations reduced bioactive GA levels in rice and potentiating the function of DELLA proteins in wheat (Colebrook *et al.*, 2014; Hedden, 2003; Van De Velde *et al.*, 2017). The DELLA proteins serve as a GA signalling negative regulator to repress plant growth (Davière and Achard, 2016; Phokas and Coates, 2021). SLR1 is the only DELLA protein in rice, as DELLA protein, it features a conserved C-terminal GRAS domain implicated in protein–protein interactions or transcriptional regulation, and an N-terminal DELLA (Asp-Glu-Leu-Leu-Ala) domain that binds to the rice GA receptor GIBBERELLIN INSENSITIVE DWARF1 (GID1) (Daviere and Achard, 2016). The formation of the GA-GID1-SLR1 complex is followed by the degradation of SLR1 with the Skp1-Cullin-F-box (SCF) E3 ubiquitin-ligase complex via 26S proteasome (Murase

et al., 2008). DELLAs are not only essential for plant growth and development, but also play key roles in regulating plant responses to biotic and abiotic stresses (Khan *et al*., 2022). Reduced GA content results in the accumulation of SLR1, which prevents the degradation of the ABA receptor Pyrabactin Resistance 1-Like 10 (PYL10) by competitively binding to the co-activator of anaphase-promoting complex Tillering and Dwarf 1 (TAD1), thereby enhancing ABA response and drought tolerance (Liao *et al*., 2023). Moreover, OsNAC120 plays a central role in negatively regulating drought tolerance by promoting GA biosynthesis and inhibiting ABA biosynthesis, establishing a balance between GA-mediated plant growth and ABA-regulated drought tolerance. Meanwhile, SLR1 interacts with OsNAC120 to impede its transactivation ability (Xie *et al*., 2023). Previous studies have concentrated on the crosstalk of GA and ABA signals, which synergistically regulate drought tolerance in plants. Therefore, the role of the GA-DELLAs module in plants' drought tolerance remains to be clarified.

Sucrose, as a primary carbon source and osmosis substance, plays a crucial role in plant growth and development. It promotes root growth and development, facilitates starch accumulation and participates in plant responses to abiotic stresses (Stein and Granot, 2019; Zhang *et al*., 2017). Water deficit induces the expression of sucrose transporters *AtSWEET11* and *AtSWEET12*, enhancing tolerance to abiotic stresses by increasing sucrose transport from shoots to roots in *Arabidopsis* (Durand *et al*., 2016). The phosphorylation of AtSWEET11 and AtSWEET12 further promotes sucrose transport from shoots to roots under drought stresses (Chen *et al*., 2022). In addition, sucrose induces SUCROSE NON-FERMENTING1 RELATED KINASE1 α subunit (SnRK1α) accumulation to phosphorylate and stabilize SPEECHLESS (SPCH), a master regulator of stomatal development, subsequently inducing epidermal cell differentiation into stomatal cells (Han *et al*., 2022). Sucrose synthesis (SUS) and sucrose invertase (INV) catalyse sucrose decomposition (Funfgeld *et al*., 2022). In maize, overexpression of *ZmSUS1* has been shown to increase drought resistance by regulating sucrose metabolism and soluble sugar content (Xiao *et al*., 2024). Despite these advances, the mechanistic understanding of sucrose's role in drought tolerance remains fragmentary and the underlying relationship of GA and sucrose is unknown.

Here, we showed that OsBURP3, a plant-specific BURP domain-containing protein, plays an essential role in GA-mediated drought response as a key interactor of SLR1. Under drought conditions, the expression of SLR1 is induced, leading to a reduction in the abundance of drought-negative regulator OsBURP3, thereby enhancing drought tolerance. Interestingly, OsBURP3 fine regulates the nucleocytoplasmic translocation of OsSUS1 by physical interaction, consequently affecting sucrose metabolism in rice. We also found that obstructing OsSUS1 transport increases sucrose levels in plants, which in turn leads to stomatal closure. More importantly, we further confirmed the involvement of the DELLA-BURP-SUS regulatory axis in maize implying a conservative mechanism of drought tolerance in crops.

Results

Exogenous GA treatment reduces drought tolerance by degrading SLR1

To investigate the role of GA in regulating drought tolerance in rice, we performed the treatment assay with exogenous GA and paclobutrazol (PAC, GA biosynthesis inhibitor). The results showed that GA-treated plants exhibited significantly decreased survival rates, whereas PAC-treated plants exhibited increased survival rates compared to Mock-treated plants under PEG6000 treatment or drought stress (Figure 1a,b; Figure S1a,b). Plants commonly employ stomatal closure as a strategy to mitigate water loss. Previous studies have shown that GA is a signal that induce stomata formation in *Arabidopsis* hypocotyls, and it also reduces sensitivity of guard cells to ABA, leading to stomatal open and decreased drought tolerance in tomato (Nir *et al*., 2017; Saibo *et al*., 2003). Scanning electron microscopy (SEM) was used to examine changes in stomatal morphology in wild-type (WT) plants under different GA levels. The data revealed that the stomatal aperture of GA-treated plants was significantly higher than that of Mock-treated plants under drought stress, while PAC-treated plants exhibited a significantly lower stomatal aperture compared to Mock-treated plants under both normal and drought stress (Figure 1c,d). Statistically analysis of stomatal density under normal and drought stress showed that GA had no significant impact on stomatal density (Figure S1c). Additionally, we examined the abundance of endogenous SLR1 proteins in the leaves of Mock-, GA- and PAC-treated plants. SLR1 protein levels were reduced in GA-treated plants, but accumulated in PAC-treated plants compared to Mock-treated plants (Figure 1e; Figure S1d). These results indicate that the survival rate of rice plants under drought stress is positively correlated with the abundance of SLR1 protein (Figure S1e).

Three homozygous *SLR1* overexpressing lines (OE-SLR1) driven by the maize *ubiquitin* promoter in the *Nipponbare* background

Figure 1 Exogenous GA treatment negatively regulates drought tolerance by degrading SLENDER RICE 1 (SLR1). (a, b) Phenotype and survival rates of gibberellin (GA)- and PAC-treated plants under the PEG6000 treatment. Mock as the control without hormone treatment. Data are mean ± SD ($n = 3$). Significant differences tested using Student's unpaired two-tailed *t*-tests. Scale bars, 10 cm. (c) Scanning electron microscopy images of leaf epidermal stomata of WT plants with different treatments under normal and drought stress. Scale bars, 5 μm. (d) Stomatal aperture in WT plants with different treatments under normal and drought stress. Data are mean ± SD ($n \geq 70$). Significant differences tested using Student's unpaired two-tailed *t*-tests. (e) Western blot showing the protein level of SLR1 in Mock-, GA- and PAC-treated plants. Anti-actin as an internal control. RbcL serves as a loading control. (f, g) Phenotype and survival rates of OE-SLR1 lines under drought treatment. WT as control. Data are mean ± SD ($n = 3$). Significant differences tested using Student's unpaired two-tailed *t*-tests. Scale bars, 10 cm. (h) Scanning electron microscopy images of leaf epidermal stomata of OE-SLR1 lines and WT plants under normal and drought stress. Scale bars, 5 μm. (i) Stomatal aperture in OE-SLR1 lines and WT plants under normal and drought stress. Data are mean ± SD ($n \geq 70$). Significant differences tested using Student's unpaired two-tailed *t*-tests. (j) Relative protein level of SLR1 in three independent OE-SLR1 lines. (k) Relative expression level of *SLR1* response to PEG6000 without and with GA treatment in different processing times. Data are mean ± SD ($n = 3$). (l) Relative protein levels of SLR1 responses to PEG6000 treatment or water in different processing times.

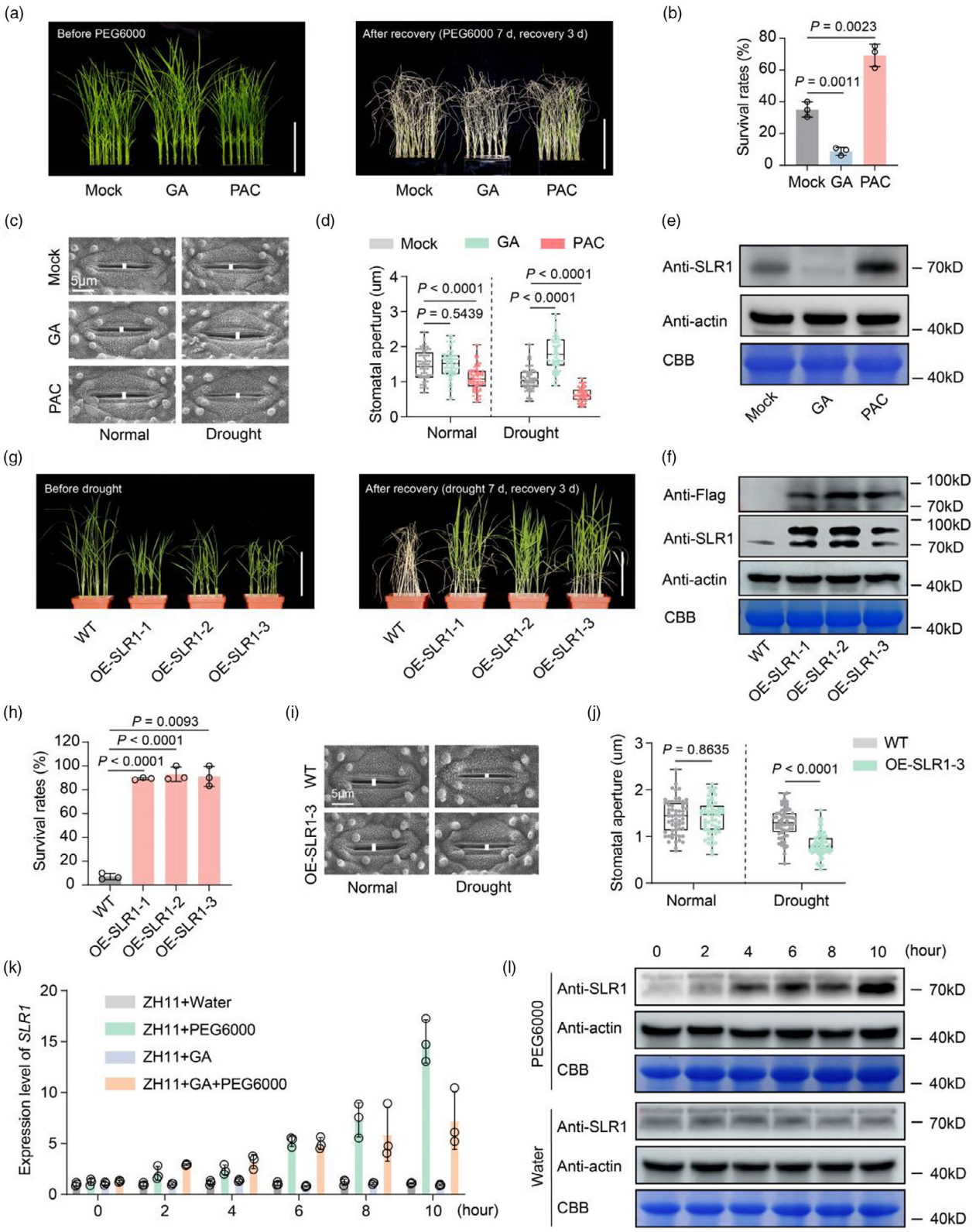

were generated to investigate the role of SLR1 in drought tolerance (Figure S2a,b). Quantitative reverse transcription quantitative polymerase chain reaction (qRT-PCR) confirmed a significant increase in *SLR1* transcription levels in the OE-SLR1 lines (Figure S2c). The accumulation of SLR1 protein in these lines was verified using Flag and specific SLR1 antibodies by Western blot (Figure 1f). Three independent OE-SLR1 lines exhibited significantly enhanced drought tolerance compared to the WT

plants (Figure 1g,h). Similar to PAC-treated plants, the OE-SLR1 lines displayed a significantly reduced stomatal aperture compared to WT under drought stress (Figure 1i,j). Consistently, no significant differences in stomatal density were observed between WT plants and OE-SLR1 lines under both normal and drought stress (Figure S2d). Proline has been recognized as a multi-functional molecule that accumulates in high concentrations in response to various abiotic stresses (Kavi Kishor and Sreenivasulu *et al*., 2013). We found that the OE-SLR1 lines accumulated more free proline compared to WT plants under drought stress, confirming the positive role of *SLR1* in drought tolerance in rice (Figure S2e).

To clarify whether the accumulation of SLR1 resulted from the regulation at the transcriptional or translational levels, we analysed the influence of the relative amount of SLR1 on mRNA and protein levels in the WT plants under drought. The results exhibited upregulated *SLR1* expression and increased protein accumulation under PEG6000 treatment, suggesting *SLR1* positively respond to drought stress (Figure 1k,l). Furthermore, *SLR1* transcription levels were not affected by exogenous GA treatment under both water and PEG6000 treatment, indicating that GA treatment inhibits drought tolerance by affecting SLR1 protein levels rather than its transcription (Figure 1k). Collectively, these findings demonstrate that SLR1 plays a crucial role in responding to drought stress and enhancing drought tolerance in rice.

SLR1 interacts with OsBURP3 to regulate its abundance

The function of SLR1 mainly relies on its interactions with diverse classes of regulatory proteins (Daviere and Achard, 2016). To gain insights into the mechanism of SLR1 action, we conducted a yeast two-hybrid (Y2H) assay to screen for SLR1 interactors. Considering the strong self-transactivation activity of SLR1 in yeast cells, 50 mM 3-aminotriazole (3-AT, a competitive inhibitor of the HIS3 enzyme) was used as an inhibitor (Figure S3a). Among the interactors, OsBURP3 (BURP domain-containing protein 3), a member of the plant-specific BURP domain protein family, was abundantly identified and is known to encode a dehydration-responsive protein (Table S1). Phylogenetic analysis and sequence alignment revealed that OsBURP3 is closely related to AtRD22, a negatively regulator involved in drought tolerance in *Arabidopsis* (Harshavardhan *et al*., 2014) (Figures S4 and S5; Table S2). The interaction between SLR1 and full-length OsBURP3 was further investigated in yeast. Co-transformants of pGBKT7-SLR1 and pGADT7-OsBURP3 grew on SD/-Trp/-Leu/-His/-Ade plates containing 50 mM 3-AT, while the control transformants did not grow (Figure 2b). Similarly, co-transformants of pGADT7-SLR1 and pGBKT7-OsBURP3 also grew on SD/-Trp/-Leu/-His/-Ade plates, confirming the interaction in yeast again (Figure S3b). To determine which domain of SLR1 attributes to the interactions with OsBURP3, we divided SLR1 into N-terminal (DELLA domain) and C-terminal (GRAS domain) truncations (Figure 2a). The results showed that both truncated proteins interacted with OsBURP3 in yeast cells (Figure 2b). Meanwhile, the bimolecular fluorescence complementation (BiFC) assay in rice protoplasts established that the interactions specifically occurred in the nucleus (Figure 2c). Split-luciferase complementation imaging (LCI) assays in *N. benthamiana* further confirmed the interaction, as co-transformation with cLUC-OsBURP3 and nLUC-SLR1 produced strong luciferase signals, indicating that the interactions indeed occurred in plants (Figure 2d). Additionally, the interaction was validated by co-immunoprecipitation (Co-IP) in vivo (Figure 2e). Collectively, these results suggest that SLR1 interacts with OsBURP3 in rice nucleus.

To investigate the regulatory effect of SLR1 on OsBURP3, we firstly examined the transcriptional levels of *OsBURP3* in OE-SLR1 line. qRT-PCR results showed that *OsBURP3* transcriptional levels were unchanged in the three OE-SLR1 lines compared to WT plants under both normal and drought stress (Figure S6a). Similarly, no significant differences in *OsBURP3* transcriptional levels were observed between GA-treated and Mock-treated plants, regardless of drought stress (Figure S6b). These findings indicate that both the abundance of SLR1 and drought treatment do not affect *OsBURP3* transcription. To further explore the potential effect of SLR1 on OsBURP3 at the protein level, we measured SLR1 and OsBURP3 protein levels in OE-OsBURP3 lines under GA and PAC treatments. After GA treatment, SLR1 protein levels gradually decreased, while OsBURP3 protein levels progressively increased (Figure 2f). Conversely, PAC treatment resulted in increased SLR1 abundance over time, accompanied by a reduction in OsBURP3 protein levels (Figure 2f). To provide additional biochemical evidence, an in vitro degradation assay was conducted. The results demonstrated that OsBURP3-maltose-binding protein (MBP) fusion protein (OsBURP3-MBP) was degraded faster when incubated with extracts from *SLR1* overexpressing lines than that incubated with extracts from WT plants (Figure 2g,h). These results suggest that SLR1 negatively regulates OsBURP3 abundance at the post-transcriptional level.

OsBURP3 negatively regulates drought tolerance in rice

To examine the expression pattern of *OsBURP3*, we analysed its expression across various tissues in WT plants. The results showed that *OsBURP3* was constitutively expressed in all the investigated tissues, with particularly high levels in the leaves (Figure 3a). Furthermore, transient expression of OsBURP3 fused with a green fluorescent protein (GFP) tag in rice protoplasts and *N. benthamiana* demonstrated that OsBURP3 was localizes to the nucleus, suggesting its functional role in this compartment (Figure 3b; Figure S7b). A previous study reported that the BURP domain was a crucial determinant for the subcellular localization of BURP family proteins (Wang *et al*., 2012). To investigate the role of the BURP domain in OsBURP3 localization, we analysed the subcellular localization of truncated OsBURP3 proteins in rice protoplasts and *N. benthamiana* (Figure S7a). The results showed that truncation or deletion of the BURP domain weakened nuclear localization signals (OsBURP3$^{1\text{-}323}$ GFP and OsBURP3$^{1\text{-}212}$ GFP), whereas retaining the BURP domain resulted in strong nuclear localization (OsBURP3$^{213\text{-}429}$ GFP) (Figure S7c,d). These results indicate that the BURP domain is essential for the localization of OsBURP3.

To get insight into the function of *OsBURP3*, the knockout lines were generated using a CRISPR/Cas9 system in the *japonica* rice cultivar Zhonghua11 (ZH11) background. Two loss-of-function lines (*osburp3-1* and *osburp3-2*) with 1-bp and 58-bp deletions in the third exon of *OsBURP3* were identified by sequencing (Figure S8a,b). Additionally, three homozygous overexpression lines fused Flag and Myc tag were obtained, named OE-OsBURP3-1, OE-OsBURP3-2 and OE-OsBURP3-3. qRT-qPCR and Western blot analyses confirmed that both transcriptional and translational levels of OsBURP3 were significantly higher in three OE-OsBURP3 lines compared to WT plants (Figure S8c,d). Subsequently, two-week-old seedlings of homozygous transgenic plants (T_2

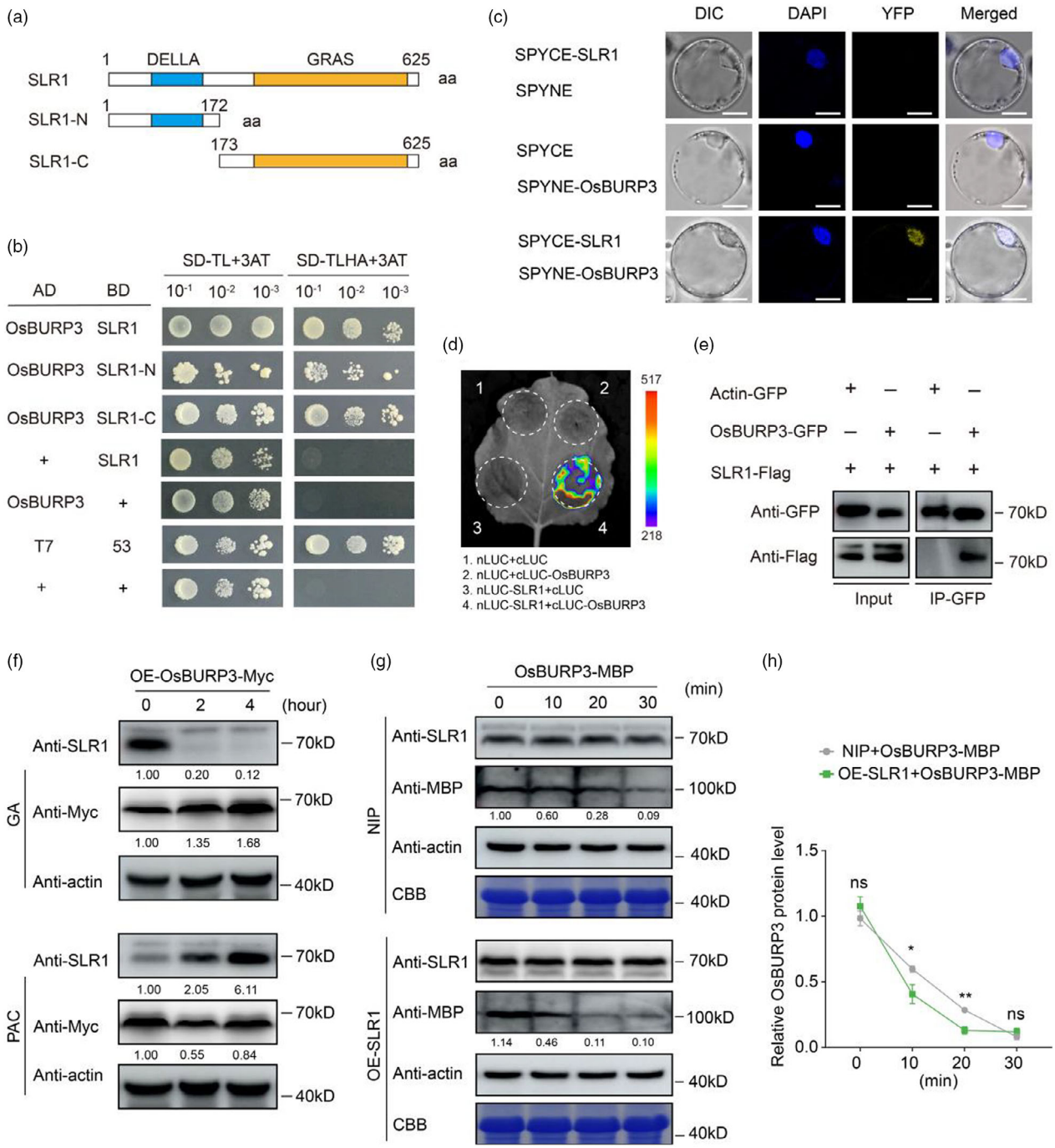

Figure 2 SLENDER RICE 1 (SLR1) interacts with OsBURP3 to regulate its abundance. (a) Schematic diagrams of a truncated version of SLR1 used in Y2H assay. SLR1-N represents the N-terminal (1–172 aa) of SLR1, and SLR1-C represents the C-terminal (173–725 aa) of SLR1. (b) Y2H assay exhibited the interaction between SLR1 and OsBURP3, the control combinations are indicated. BD, DNA-binding domain. AD, activation domain. SD, yeast dropout culture medium. T, Trp; L, Leu; H, His; A, Ade. (c) BiFC assay exhibited the interaction between SLR1 and OsBURP3 in rice protoplasts. DAPI as a nuclear marker. Scale bars, 5 μm. (d) LCI assay exhibited the interaction between SLR1 and OsBURP3 in *N. benthamiana*. nLUC and cLUC were used as a negative control. (e) Co-IP assay of SLR1 with OsBURP3 in the transgenic plant. (f) In vivo degradation assay, relative protein abundance of SLR1 and OsBURP3 in OE-OsBURP3-Myc lines with GA and PAC treatment. Anti-actin as an internal control. Values above panels indicate signal strength for SLR1 and Myc in arbitrary units determined by image J. (g, h) In vitro degradation assay, relative protein abundance of SLR1 and OsBURP3 in recombinant proteins of OsBURP3-MBP co-incubated with total protein from NIP or OE-SLR1 lines. Anti-actin as an internal control. RbcL as a loading control. Values above panels indicate the signal strength for MBP in arbitrary units determined by image J. Data are mean ± SD ($n = 2$). Asterisks indicate significant differences (*$P < 0.05$, **$P < 0.01$, Student's unpaired two-tailed *t*-tests).

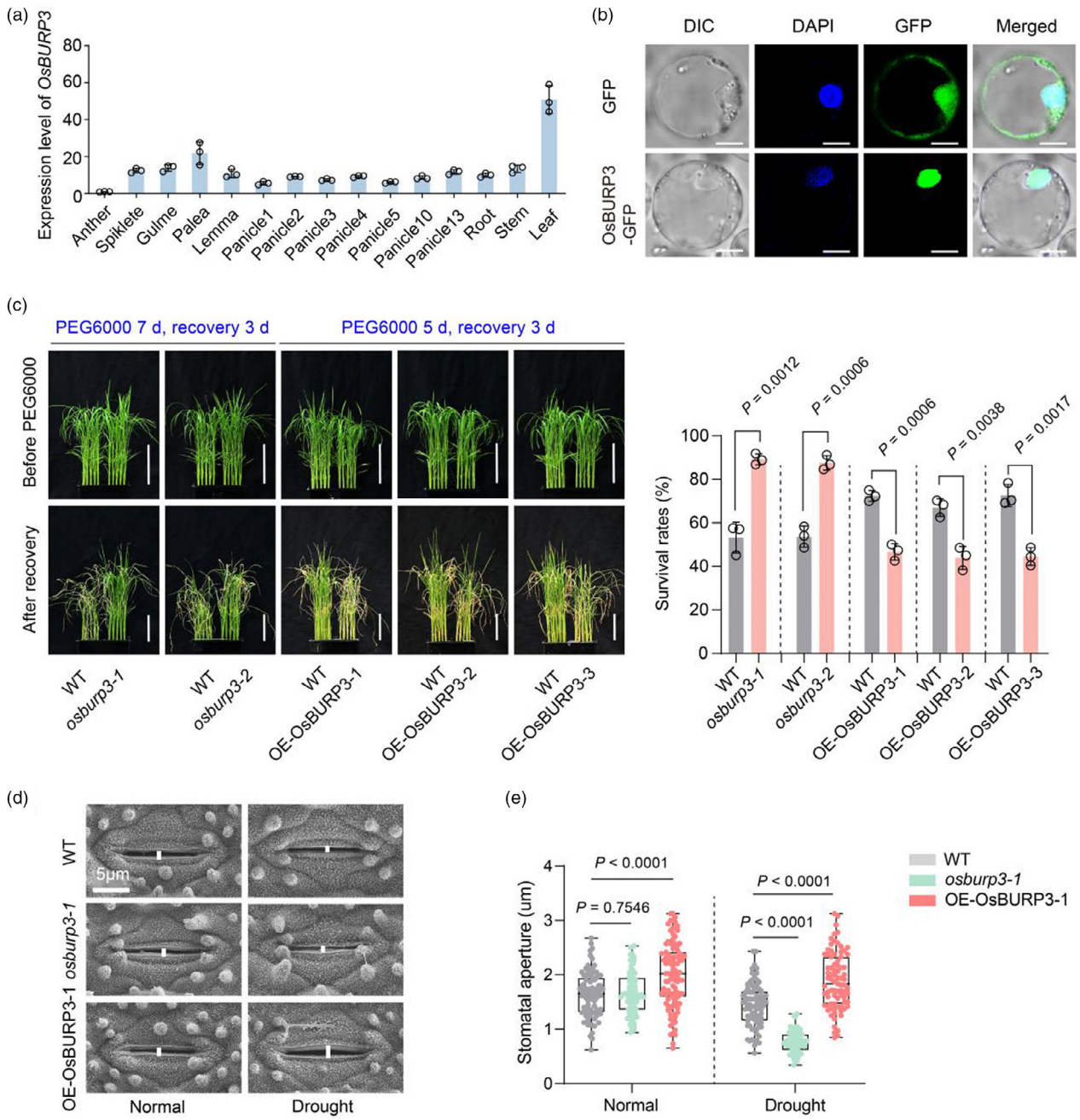

Figure 3 *OsBURP3* negatively regulates drought tolerance. (a) Expression pattern of *OsBURP3* in different tissues of WT plants. Data are mean ± SD ($n = 3$). (b) Detection of subcellular localization of OsBURP3-GFP in rice protoplasts. DAPI was used as a nuclear marker. Scale bar, 5 μm. (c) Phenotype and survival rates of *OsBURP3* transgenic lines and WT plants under drought treatment. Data are mean ± SD ($n = 3$). The statistical significance was determined by Student's unpaired two-tailed *t*-tests. Scale bars, 10 cm. (d) Scanning electron microscopy images of leaf epidermal stomata of *OsBURP3* transgenic lines and WT plants under normal and drought stress. Scale bars, 5 μm. (e) Stomatal aperture in *OsBURP3* transgenic lines and WT plants under normal and drought stress. Data are mean ± SD ($n \geq 70$). Significant differences tested using Student's unpaired two-tailed *t*-tests.

generation) and WT plants were exposed to 20% PEG6000 for drought treatment. Statistical analysis showed that *osburp3* mutant lines exhibited significantly higher survival rates compared to WT, whereas OE-OsBURP3 lines displayed the opposite trend (Figure 3c). Similar results were observed when these transgenic plants were exposed to soil drought treatment in pots (Figure S8e, f). These results suggest that *OsBURP3* negatively regulates the drought tolerance in rice.

To further elucidate the role of *OsBURP3* in drought tolerance, stomatal aperture and density were measured using SEM. The results showed that under drought stress, stomatal aperture in *osburp3-1* mutant was significantly lower than in WT plants, whereas OE-OsBURP3-1 plants had a significantly higher stomatal aperture compared to WT under both normal and drought stress (Figure 3d,e). However, no significant differences in stomatal density were observed between *OsBURP3* transgenic lines and

WT plants under either condition (Figure S8g). Furthermore, we measured the free proline contents of WT and *OsBURP3* transgenic plants under normal and drought condition. Results showed less proline was accumulated in the OE-OsBURP3 lines than those in the WT plants and knockout lines under drought stress, implying less drought tolerance capacity of OE lines (Figure S8h). Overall, these findings suggest that *OsBURP3* regulates drought tolerance in rice by modulating stomatal aperture.

To assess whether the enhanced drought tolerance of *osbrup3* mutant lines comes at the cost of growth and yield, a detailed yield-trait evaluation was conducted over two seasons. Field experiments revealed that *osburp3* mutant lines had significantly increased grain length and width, whereas OE-OsBURP3 lines did not show significant differences compared to WT plants (Figure S9a,b). Both knockout and overexpression lines exhibited increased the 1000-grain weight compared to WT plants (Figure S9c). The panicle number per plant was slightly lower in *osburp3* mutant lines compared to OE-OsBURP3 lines and WT plants (Figure S9d). However, grain yield per plant was not significantly different across all transgenic plants (Figure S9e). These results indicate that the gain of function in *osburp3* mutant lines enhances drought tolerance without compromising yield, implying the potential application value in rice.

SLR1 competed with OsSUS1 to interact with OsBURP3 in the nucleus

To elucidate the in-depth mechanism by which OsBURP3 regulates drought tolerance in rice, we performed an IP assay using *OsBURP3* overexpression lines tagged with Flag and Myc, followed by liquid chromatography–tandem mass spectrometry (LC–MS/MS) to identify potential interacting proteins. Sucrose synthase OsSUS1, a key enzyme involved in sugar metabolism, was identified as a candidate interactor (Table S3). To confirm the interaction between OsBURP3 and OsSUS1, firstly, the Y2H assays were performed. The yeast cells carrying both pGBKT7-OsBURP3 and pGADT7-OsSUS1 constructs grew on SD/-Trp/-Leu/-His/Ade plates, whereas control transformants did not grow (Figure 4b). Further analysis showed that truncated OsBURP3 proteins (OsBURP3$^{1\text{-}212}$ and OsBURP3$^{213\text{-}429}$) failed to interact with OsSUS1, indicating that the full-length OsBURP3 is required for binding (Figure 4a,b). BiFC assay also showed that aside from the two truncated proteins of OsBURP3 and negative controls, strong YFP fluorescence signals from complete OsBURP3 and OsSUS1 were observed in the nucleus, confirming the interaction between OsBURP3 and OsSUS1 in rice protoplasts (Figure 4c). Additionally, a pull-down assay showed that OsBURP3-MBP but not MBP alone interacted with OsSUS1-His (Figure 4d). In the LCI assay, co-expression of cLUC-OsBURP3 and nLUC-OsSUS1 in *N. benthamiana* generated strong LUC signals, further confirming that the interaction indeed existed in planta (Figure 4e). These results demonstrate that OsBURP3 interacts with OsSUS1 in the nucleus.

To further investigate the relationship among SLR1, OsBURP3 and OsSUS1, a yeast three-hybrid (Y3H) assay was performed. The results showed that OsBURP3 could interact with SLR1 when OsSUS1 expression was induced by methionine (Met) in yeast. However, OsBURP3 did not interact with OsSUS1 when SLR1 expression was induced by Met (Figure 4f). Consistent results were observed when the self-activation activity of SLR1 was inhibited by 50 or 60 mM 3AT (Figure S10). These findings suggest that SLR1 disrupts the interaction between OsBURP3 and OsSUS1. Additionally, pull-down assays showed that OsSUS1-His was successfully pulled down by OsBURP3-MBP, but its abundance significantly decreased when SLR1-GST was present (Figure 4g). The LCI assay in *N. benthamiana* also confirmed that the LUC signals resulting from the interaction between cLUC-OsBURP3 and nLUC-OsSUS1 were significantly attenuated in the presence of SLR1 compared to the control flag protein (Figure 4h,i). Collectively, these results strongly suggested that SLR1 competitively interacted with OsBURP3 to orchestrate its association with sucrose synthase OsSUS1 in rice.

GA-SLR1-OsBURP3 module regulates the nucleocytoplasmic trafficking of OsSUS1

Plant sucrose synthase isozymes are mainly located in the cytosol or adjacent to the plasma membrane (Koch, 2004; Stein and Granot, 2019). Our finding demonstrated that OsBURP3 physically interacted with OsSUS1 in the nucleus (Figure 4c), prompting us to investigate whether OsBURP3 recruits OsSUS1 into the nucleus from the cytosol. To examine the subcellular localization of OsSUS1, GFP-tagged OsSUS1 was transiently expressed under the 35S promoter in rice protoplasts. GFP signals were primarily detected in the cytosol with minimal presence in the nucleus (Figure 5a,b). Interestingly, upon treatment with exogenous GA, nuclear accumulation of OsSUS1-GFP significantly increased (Figure 5a,b). Similar results were observed when OsSUS1-GFP was transiently expressed in *N. benthamiana* (Figure S11a–d). These results suggest that GA signalling regulates the nucleocytoplasmic translocation of OsSUS1. Considering the competitive interaction between SLR1 and OsSUS1, we co-expressed SLR1-RFP and OsSUS1-GFP in rice protoplasts under Mock and GA treatments. Results showed increased nuclear GFP signals and decreased SLR1-RFP signals upon GA treatment (Figure 5c,d). These findings imply that GA and decreased SLR1 protein levels efficiently trigger the translocation of OsSUS1 from the cytosol into the nucleus.

To further confirm the effect of GA on OsSUS1 translocation, Western blot analysis was performed on cytosolic and nuclear fractions of WT plants with and without GA treatment. The results revealed a significant increase in nuclear OsSUS1 protein levels and a decrease in cytosolic levels in GA-treated plants compared to Mock-treated controls (Figure 5e). In addition, in the *osburp3* mutant lines, OsSUS1 protein levels were higher in the cytosol and lower in the nucleus compared to WT plants and two OE-OsBURP3 lines, supporting the role of OsBURP3 in facilitating OsSUS1 nuclear translocation (Figure 5f; Figure S12a,b).

For additional cytological evidence, an immunogold labeling assay using Anti-OsSUS1 antibodies was conducted, followed by high-resolution transmission electron microscopy. The number of gold particles decreased in the nucleus of *osburp3* mutant lines, but visibly increased in OE-*OsBURP3* lines compared to WT, suggesting that OsBURP3 contributed to the translocation of OsSUS1 from the cytosol to the nucleus (Figure 6). More gold particles were also observed in the nucleus of GA-treated plants compared to Mock-treated plants (Figure S13a–d). Additionally, we also found a decrease of gold particles in the nucleus of the OE-SLR1 lines compared to WT (Figure S11e–g). These findings support that the GA-SLR1-OsBURP3 axis contribute to the nucleocytoplasmic translocation of OsSUS1.

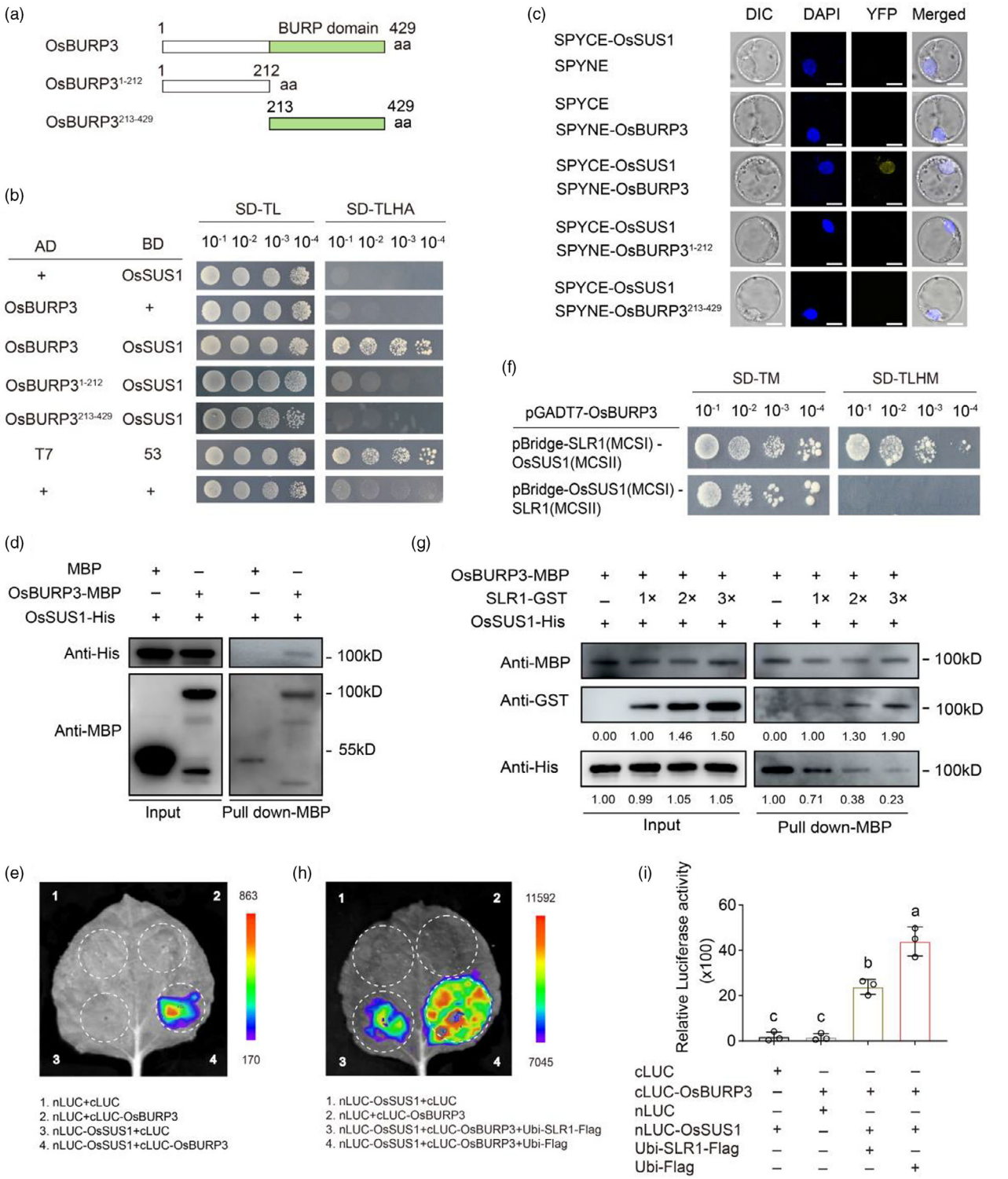

Figure 4 SLR1 competed with OsSUS1 to interact with OsBURP3. (a) Schematic diagrams of a truncated version of OsBURP3 used in Y2H assay and BiFC assay. (b) Y2H assay exhibited the interaction between OsBURP3 and OsSUS1. BD, DNA-binding domain. AD, activation domain. SD, yeast dropout culture medium. T, Trp; L, Leu; H, His; A, Ade. (c) BiFC assay showed the interaction of OsBURP3 with OsSUS1 in rice protoplasts. DAPI as a nuclear marker. Scale bar, 5 μm. (d) Pull-down assay exhibited the interaction between OsBURP3 and OsSUS1. (e) LCI assay showed that OsBURP3 interacts with OsSUS1 in *N. benthamiana*. nLUC and cLUC were used as a negative control. (f) Y3H assay showed that SLR1 competed with OsSUS1 to interact with OsBURP3 in yeast. SD, yeast dropout culture medium. T, Trp; L, Leu; H, His; M, Met. (g) Pull-down assay confirmed the interaction between OsBURP3 with OsSUS1, which was restrained by SLENDER RICE 1 (SLR1). The signal strength was calculated by image J. (h, i) LCI assay showed that SLR1 disrupted the interaction between OsBURP3 with OsSUS1 in *N. benthamiana* (h). Relative luciferase activity was statistically by ImageJ (i). Data are mean ± SD ($n = 3$). Different letters indicate significant differences tested using one-way ANOVA/Tukey's multiple range test ($P < 0.05$).

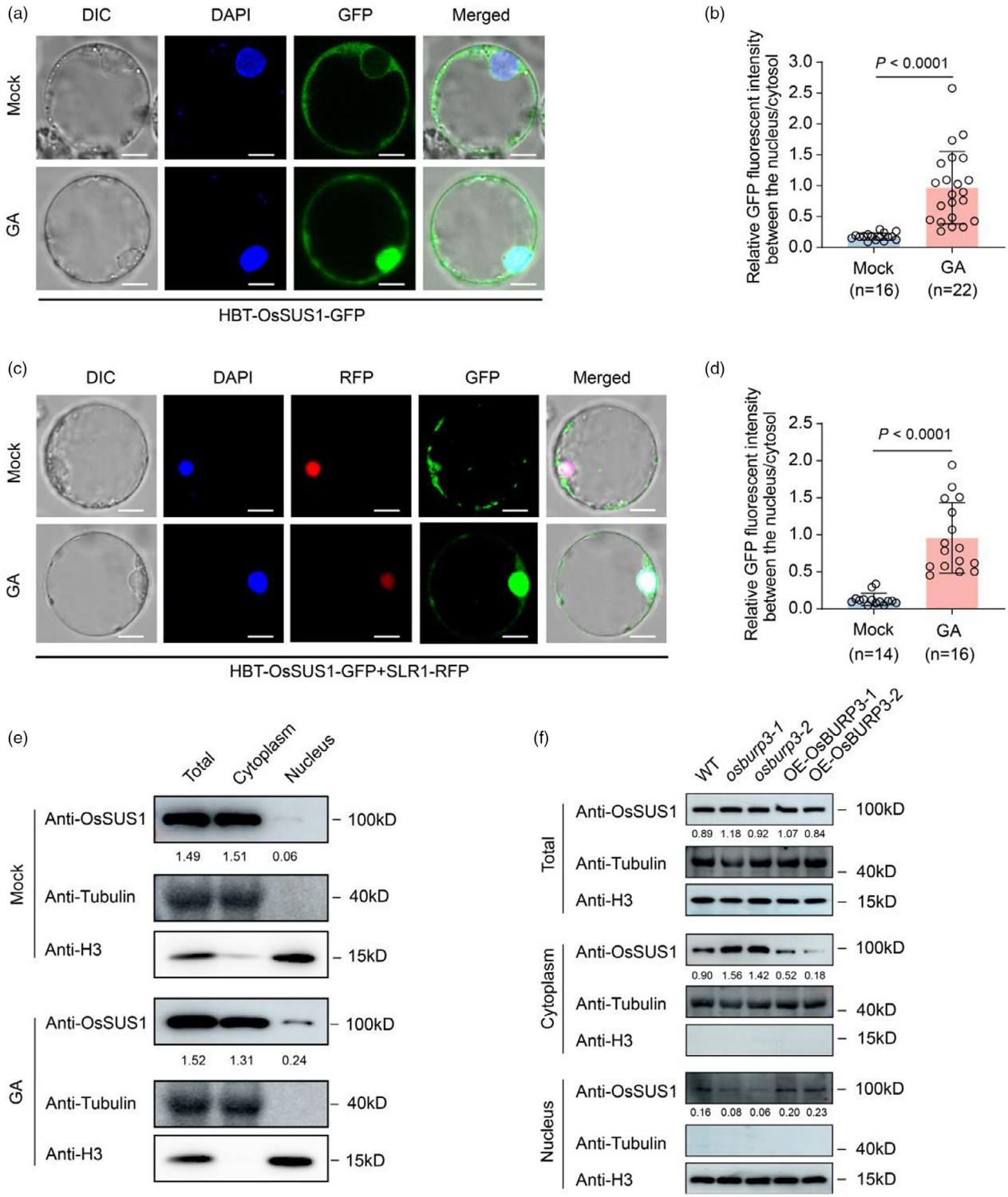

Figure 5 GA signalling mediated-OsBURP3 regulates the subcellular localization of OsSUS1. (a, b) Different nucleus accumulation (a) and quantification (b) of relative GFP fluorescent signal intensity between the nucleus and cytoplasm of OsSUS1-GFP with and without gibberellin (GA) treatment. Data are mean ± SD ($n \geq 16$). The statistical significance was determined by Student's unpaired two-tailed *t*-tests. DAPI as a nuclear marker. Scale bar, 5 μm. (c, d) Different nucleus accumulation (c) and quantification (d) of relative GFP fluorescent signal intensity between the nucleus and cytoplasm of OsSUS1-GFP when competitive with SLENDER RICE 1 (SLR1)-RFP in rice protoplasts. Data are mean ± SD ($n \geq 14$). The statistical significance was determined by Student's unpaired two-tailed *t*-tests. DAPI as a nuclear marker. Scale bar, 5 μm. (e) Detection of OsSUS1 in the total, cytoplasm and nucleus fraction in GA-treated plants. Anti-Tubulin and Anti-H3 were used as internal control. Values above panels indicate the ratio of OsSUS1 with the internal control signal. The signal strength was calculated by image J. (f) Detection of OsSUS1 in the total, cytoplasm and nucleus fractions from *OsBURP3* transgenic lines and WT plants. Values above panels indicate the ratio of OsSUS1 with the internal control signal. The signal strength was calculated by image J.

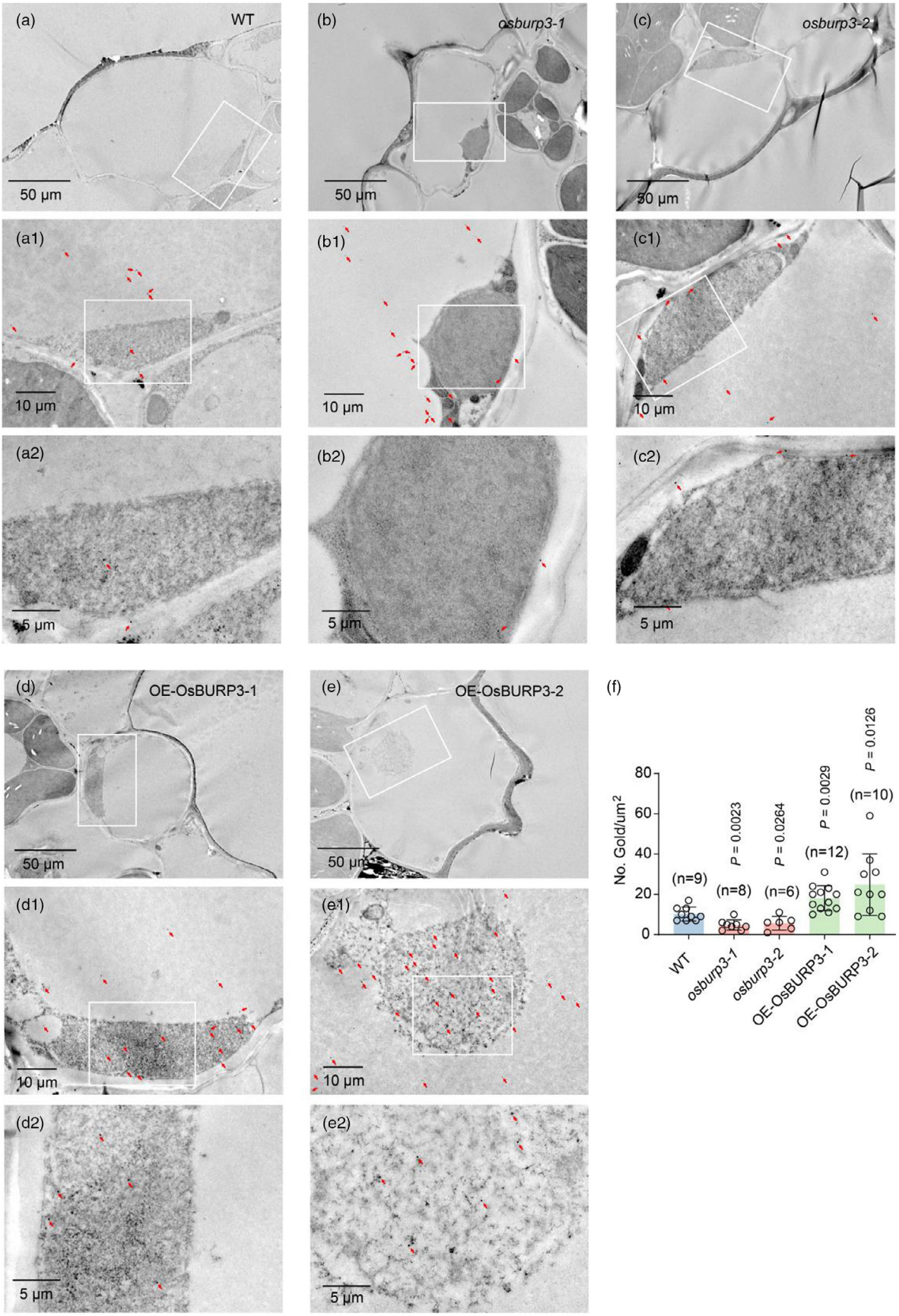
(a)
WT
50 μm
(b)
osburp3-1
50 μm
(c)
osburp3-2
50 μm
(a1)
10 μm
(b1)
10 μm
(c1)
10 μm
(a2)
5 μm
(b2)
5 μm
(c2)
5 μm
(d)
OE-OsBURP3-1
50 μm
(e)
OE-OsBURP3-2
50 μm
(f)
No. Gold/um2
80
60
40
20
0
(n=9)
(n=8)
(n=6)
(n=12)
(n=10)
P = 0.0023
P = 0.0264
P = 0.0029
P = 0.0126
WT
osburp3-1
osburp3-2
OE-OsBURP3-1
OE-OsBURP3-2
(d1)
10 μm
(e1)
10 μm
(d2)
5 μm
(e2)
5 μm

Figure 6 Immunogold labeling detection of *OsBURP3* transgenic lines and WT plants. (a–e) Immunogold labeling detection of *OsBURP3* transgenic lines and WT plants with the Anti-OsSUS1 antibodies. Middle and down images containing the border are enlargements of the frames in the upper. Scale bar, 50, 10 and 5 μm. (f) Quantitative analysis of the number of gold particles in the nucleus. Data are mean ± SD ($n \geq 6$). The statistical significance was determined by Student's unpaired two-tailed *t*-tests.

We hypothesized that OsBURP3 facilitates the cytosol-to-nucleus translocation of OsSUS1 via direct interaction. To test this, the colocalization of OsBURP3 and OsSUS1 were assessed in rice protoplasts. Interestingly, only the full-length OsBURP3 colocalized with OsSUS1 in the nucleus, while truncated OsBURP3 and negative control did not show merged signals (Figure S14a). This finding supported the notion that the full-length OsBURP3 physically interacted with OsSUS1 in the nucleus. To further confirm these results, the experiment was repeated in *N. benthamiana*. Similar results were observed, that the merged fluorescent signals specifically accumulated into the nucleus in the presence of full-length OsBURP3, but not in the presence of other truncated OsBURP3 proteins (Figure S14b). Thus, we conclude that the physical association of OsBURP3 and OsSUS1 plays a critical role in facilitating the translocation of OsSUS1 from the cytosol to the nucleus.

GA signalling influences sucrose metabolism in rice

To explore the function of OsSUS1 in rice, we analysed its expression pattern using qRT-PCR. The results showed that *OsSUS1* is primarily expressed in root, seedling and panicle tissues, suggesting its functional role in these tissues (Figure S15). Two *OsSUS1* knockout lines (*ossus1-1* and *ossus1-2*) were generated and OE-*OsSUS1* lines were obtained from Peng Lab (Fan *et al.*, 2019); all of these were confirmed by sequencing and Western blot (Figure S16a–c). Drought tolerance assays showed that the survival rates of *ossus1* mutant lines decreased, while those of the OE-OsSUS1 line increased compared to WT plants under drought conditions (Figure 7a,b). Similar results were also observed when these transgenic plants were exposed to soil drought treatment in pots (Figure S16d,e). These results suggest a positive role of *OsSUS1* in drought tolerance. We further analysed stomatal aperture and density in WT and *OsSUS1* transgenic lines. Under normal conditions, no significant differences in stomatal aperture were observed between the WT plants and *OsSUS1* transgenic lines. However, under drought stress, the stomatal aperture of the *ossus1-1* mutant was significantly higher than that of WT plants, while the aperture in the OE-OsSUS1 line was significantly lower than in WT (Figure 7c,d). Stomatal density showed no significant difference between transgenic lines and WT plants under both conditions (Figure S16f). Consistently, the free proline content was lower in the *ossus1* mutant lines than in WT plants, while OE-OsSUS1 lines exhibited significantly higher free proline levels compared to WT plants under drought stress (Figure S16g). These results suggest that *OsSUS1* may regulate drought tolerance by affecting stomatal aperture in rice.

OsSUS1 belongs to the sucrose synthase family, which catalyses the reversible transfer of a glucosyl moiety between fructose and a nucleoside diphosphate (NDP) (sucrose + NDP = NDP-glucose + fructose) (Stein and Granot, 2019). Therefore, we measured the sucrose synthase activity in *OsSUS1* transgenic plants. The data showed that the sucrose synthase activity was significantly reduced in *ossus1* mutant lines, whereas the activity of sucrose synthase increased in the OE-OsSUS1 line (Figure 7e). These results indicate that the loss-of-function of *OsSUS1* leads to a significant reduction in sucrose synthase activity in rice. Consistently, the sucrose content was lower in *ossus1* mutant lines and higher in OE-OsSUS1 lines compared to WT plants both normal and drought stress (Figure 7f). These findings imply the crucial role of *OsSUS1* in mediating drought tolerance by regulating sucrose metabolism in rice.

Given that OsBURP3 regulates the nucleocytoplasmic translocation of OsSUS1 via physical interaction, we speculated that sucrose content would also change in *OsBURP3* transgenic lines. Results showed that sucrose content was significantly decreased in OE-OsBURP3 lines, whereas significantly increased in *osburp3* mutant lines compared to WT under both normal and drought stress (Figure 7g). Previous data showed that SLR1 negatively regulated the abundance of OsBURP3, we further detected the sucrose content in OE-SLR1 lines. Similarly, under normal and drought stress, OE-SLR1 lines accumulated more sucrose than WT plants (Figure 7h). Exogenous GA treatment reduced sucrose content in ZH11 plants, whereas PAC treatment increased it under both normal and drought stress (Figure 7i). These findings inspired us to hypothesize that sucrose could improve rice drought tolerance in vitro. As expected, the survival rates of sucrose-treated WT plants under PEG6000 treatment increased progressively accompanied by increasing sucrose concentration (Figure S17a,b). These findings suggested that the sucrose content was positively associated with drought tolerance in rice. Importantly, stomatal aperture in sucrose-treated plants was significantly lower than in Mock-treated plants under drought stress, while stomatal density showed no significant differences between Mock- and sucrose-treated plants (Figure S17c–e). Overall, these observations establish a mechanistic link between GA signalling and sucrose metabolism in regulating drought tolerance in rice. The altered stomatal aperture regulated by the GA-SLR1-OsBURP3-OsSUS1 axis, which affects sucrose content, is a crucial factor contributing to drought tolerance in rice.

Discussion and conclusion

Global climate change has increased the frequency and severity of drought worldwide, particularly in drought-prone regions. Drought is the most destructive abiotic factor affecting plant growth and crop production, causing more annual yield loss than all pathogens combined (Gupta *et al.*, 2020). Over evolutionary time, plants have developed diverse strategies to survive hostile environments. However, the mechanisms by which plants sense and respond to drought especially the genes and pathways involved in ecological adaptation and crop improvement remain largely unclear (Juenger and Verslues, 2023). GAs and DELLAs play prominent roles not only in seed germination, elongation growth and flowering, but also in regulating abiotic and biotic stress responses (Achard *et al.*, 2007; Colebrook *et al.*, 2014; Yang *et al.*, 2012). We firstly investigated the role of GA signalling and its master repressor DELLAs with sucrose metabolism in drought tolerance in rice. Results demonstrate that the transcription and protein levels of *SLR1* increase under drought stress, with OE-SLR1 lines exhibiting enhanced drought tolerance.

DELLAs, also known as 'Green Revolution' genes, modulate the expression of target genes via direct protein–protein interaction with numerous transcription factors (TFs) and epigenetic regulators (Huang *et al.*, 2023). The current model proposes two primary modes of DELLA action: (1) DELLA interacts with TFs to facilitate their binding to target promoters; and (2) DELLA

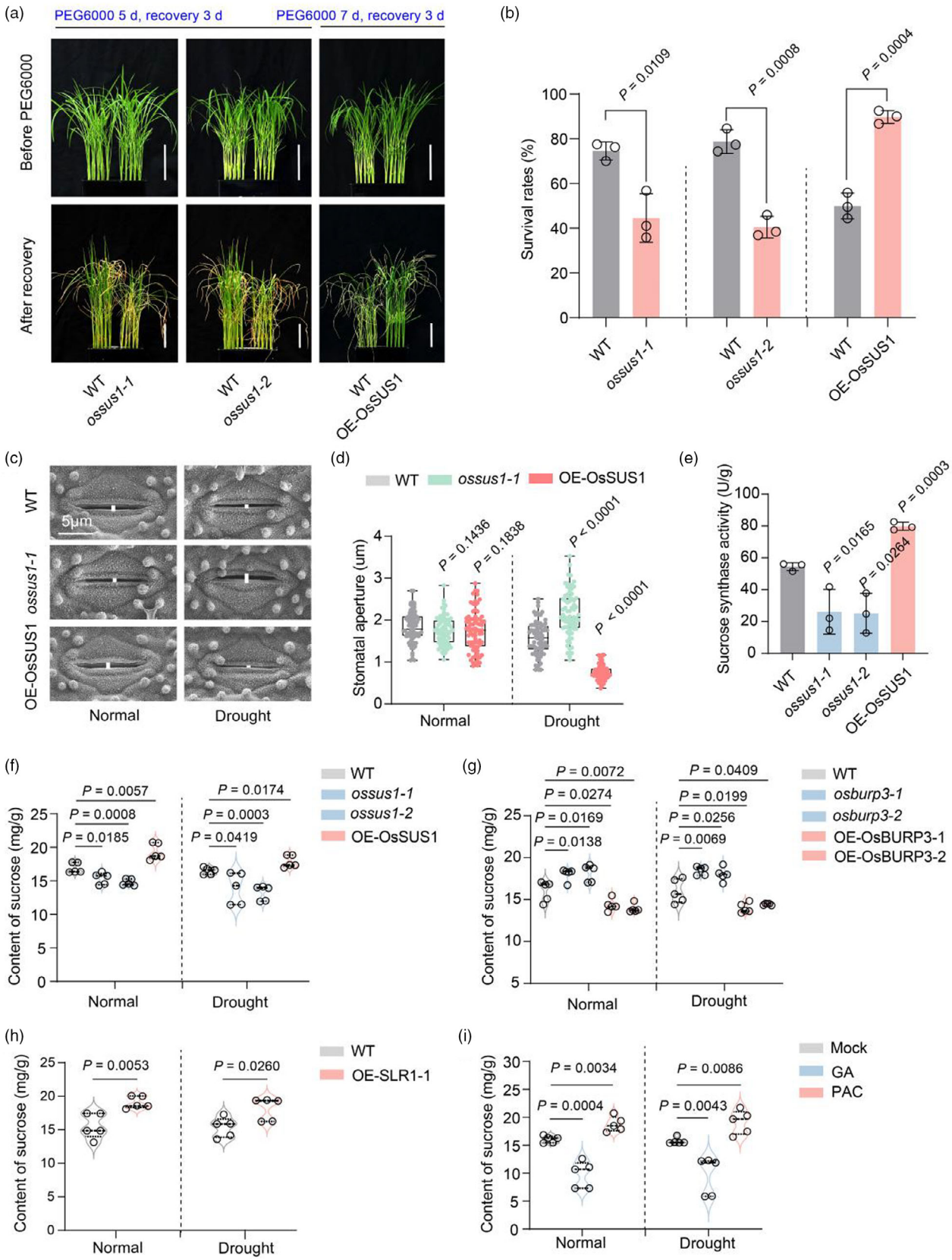

Figure 7 *OsSUS1* positively regulates drought tolerance via mediating sucrose metabolism. (a, b) Phenotype and survival rates of *OsSUS1* transgenic lines and WT plants under PEG6000 treatment. Data are mean ± SD ($n = 3$). The statistical significance was determined by Student's unpaired two-tailed *t*-tests. Scale bar, 10 cm. (c) Scanning electron microscopy images of leaf epidermal stomata of *OsSUS1* transgenic lines and WT plants under normal and drought stress. Scale bar, 5 μm. (d) Stomatal aperture in *OsSUS1* transgenic lines and WT plants under normal and drought stress. Data are mean ± SD ($n \geq 70$). Significant differences tested using Student's unpaired two-tailed *t*-tests. (e) Detection of sucrose synthase activity of *OsSUS1* transgenic lines and WT plants. Data are mean ± SD ($n = 3$). The statistical significance was determined by Student's unpaired two-tailed *t*-tests. (f–h) Examination of sucrose content of *OsSUS1* transgenic lines (f), *OsBURP3* transgenic lines (g), *SLR1* transgenic lines under normal and drought stress (h). Data are mean ± SD ($n = 5$). The statistical significance was determined by Student's unpaired two-tailed *t*-tests. (i) Examination of sucrose content of WT plants with Mock, GA and PAC treatment under normal and drought stress. Data are mean ± SD ($n = 5$). The statistical significance was determined by Student's unpaired two-tailed *t*-tests.

sequesters TFs, preventing them from binding to DNA (Huang *et al*., 2023). In this study, we found that SLR1-mediated OsBURP3 degradation contributes to drought tolerance in rice. However, the exact mechanism by which SLR1 negatively regulates OsBURP3 protein abundance remains unclear. A recent study reported that GA promotes SLR1 degradation and enhancing OsPIL14 accumulation, whereas PAC inhibits OsPIL14 accumulation, particularly under salt stress. This suggests that SLR1 might affect OsPIL14 stability (Mo *et al*., 2020). Coincidentally, a previous study showed that DELLAs negatively regulate the levels of four PIF proteins (PIF1, PIF3, PIF4 and PIF5) through the ubiquitin-proteasome system, coordinating light and GA signalling in *Arabidopsis*. DELLAs sequester PIF3 and promote its degradation, thereby reducing PIF3's binding to target genes (Li *et al*., 2016). It was proposed that the sequestration and degradation of DELLA interaction proteins by DELLAs might be a general mechanism in plants. However, as DELLAs are not E3 ubiquitin ligases, the exact process by which DELLAs mediate the degradation of interacting proteins through the ubiquitin-proteasome pathway remains speculative. It is speculated that DELLAs may cooperate with other interacting factors that facilitate post-translational modifications. Thus, determining the precise mechanism by which SLR1 triggers OsBURP3 degradation is a key goal for future studies. Our study also reports a novel working model in which DELLA competitively interacts with a non-transcription factor, OsBURP3, which was involved in the nucleocytoplasmic translocation of OsSUS1, thereby changing sucrose metabolism in rice. Our results suggest that the physical association between OsBURP3 and OsSUS1 facilitates OsSUS1's translocation from the cytosol to the nucleus, and only full-length OsBURP3 could interact with OsSUS1 in the nucleus. This interaction underscores the importance of OsBURP3 in regulating sucrose metabolism and contributes to our understanding of the GA-DELLA-BURP-SUS axis in drought tolerance. According to our findings, small amounts of OsSUS1 are distributed in the nucleus, suggesting that OsSUS1 may perform other important functions in the nucleus. Previous studies have shown that transcription factor STRESS_tolerance and GRAIN_LENGTH (OsSGL) directly inhibit the expression of OsSUS1 in the endosperm to regulate the starch and amylose content, while OsSUS1 interacts with OsSGL to release its transcriptional repression ability (Liu *et al*., 2022). Therefore, nucleocytoplasmic translocation of OsSUS1 may play an important role in the balance between plant growth and development and stress resistance.

This axis was also investigated in another important model crop, maize. We examined the survival rates of maize WT plants treated with exogenous GA and PAC under drought treatment. Consistent with findings in rice, GA-treated maize plants exhibited significantly decreased survival rates, whereas PAC-treated plants exhibited increased survival rates compared to Mock-treated controls (Figure S18a,b). Two DELLA proteins, DWARF8 and DWARF9, had been characterized previously in maize (Figure S19a). The results showed a close evolutionary relationship between ZmBURP4 or ZmBURP10 and OsBURP3 (Figures S4 and S5). Subsequently, the Y2H assays demonstrated that ZmBURP4 and ZmBURP10 interact with maize DELLA proteins DWARF8 and DWARF9 (Figure S20a). In LCI assay, the strong LUC signals from nLUC-DWARF8 and cLUC-BURP4, nLUC-DWARF8 and cLUC-BURP10, nLUC-DWARF9 and cLUC-BURP4, and nLUC-DWARF9 and cLUC-BURP10 were observed, suggesting the interactions of ZmBURP4 and ZmBURP10 with DWARF8 or DWARF9 in maize in vivo (Figure S20b–e). Based on a previous overview of sucrose synthases in plants, six SUSs in maize were cloned to detect their interactions with BURPs (Stein and Granot, 2019) (Figure S19b). Y2H analysis showed that only ZmSUS1 interacts with ZmBURP4, and ZmSUS3 interacted with ZmBURP10 (Figure S21a,b). The LCI assay also established the interactions of ZmSUS1 with ZmBURP4 and ZmSUS3 with ZmBURP10 in plants (Figure S21c,d). Given DELLA's role as a central modulator of GA signalling, we hypothesized that the DELLA-BURP-SUS module also influences sucrose metabolism during drought response in maize. Interestingly, sucrose content measurements revealed that GA treatment was decreased sucrose levels in maize plants, whereas PAC treatment significantly increased them under both normal and drought stress (Figure S21e). The positive association between sucrose content and drought tolerance was further supported by results from PAC and drought treatments, suggesting that the DWARF8(9)-ZmBURP4(10)-ZmSUS1(3) axis also contributes to drought tolerance in maize.

Combining the results from rice and maize, we presumed that this DELLA-BURP-SUS axis is a conserved module for overcoming drought stress in crops. We proposed a model to illustrate how GA and DELLA coordinate drought tolerance by regulating endogenous sucrose levels in plants (Figure 8). More importantly, *OsBURP3* knockout mutants exhibited enhanced drought tolerance without yield penalties, highlighting the potential of *BURPs* for crop improvement in rice, maize and even in other crops. Alternatively, manipulating *DELLA* promoters to enhance responses to water deficiency could be another strategy to improve drought tolerance without restricting growth under normal conditions. Importantly, the function of the GA-DELLA regulatory module in regulating growth and stress tolerance is conserved in Potato, Soybean, Cotton and other dicotyledonous crops, implying this drought tolerance pathway may be general in these species. Thus, this provides a new choice for improving the drought tolerance of these species and has important significance for breeding. Overall, our study revealed a general mechanistic

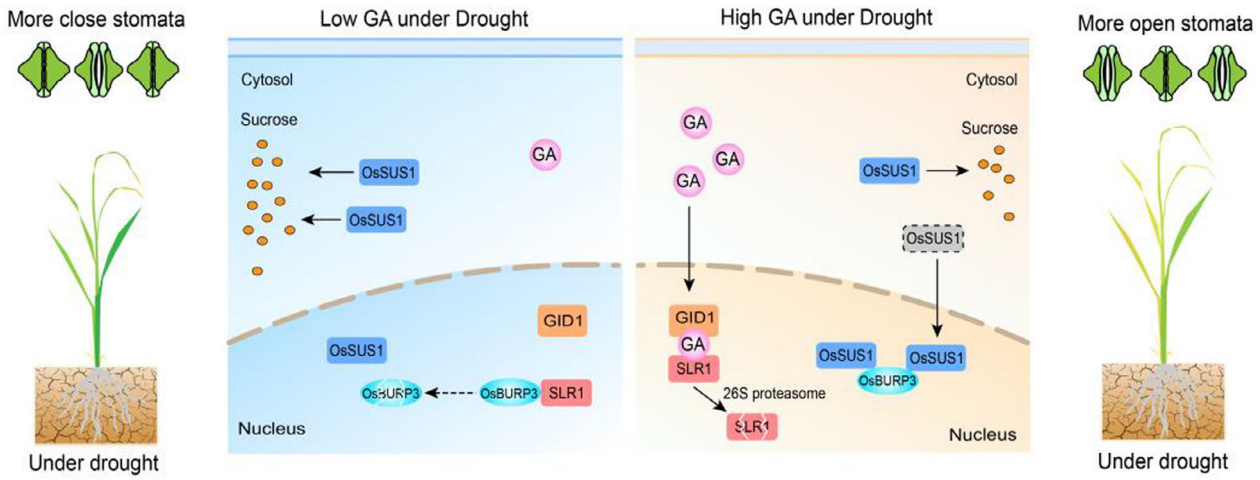

Figure 8 Proposed model for SLR1-OsBURP3-OsSUS1 axis in drought tolerance in rice. A working model for gibberellin (GA) regulates drought tolerance by sucrose metabolism in plants. In the low level of GA and under water deficiency, SLENDER RICE 1 (SLR1) is upregulated and abundant in the nucleus. Subsequently, SLR1 competes with OsSUS1 to interact with OsBURP3 thereby degrading OsBURP3. Meanwhile, OsSUS1 is mainly localized to the cytoplasm involved in sucrose metabolism consequently the higher content of sucrose leads to closing stomata and enhanced drought tolerance. However, in the high level of GA and drought conditions, SLR1 was degraded and released its interactor, OsBURP3, which recruits more OsSUS1 into the nucleus from the cytosol. Finally, the lower content of sucrose content results in an opening of stomata in leaves and gives rise to compromising drought tolerance.

framework for understanding how the DELLA-BURP-SUS module regulates sucrose metabolism to enhance drought tolerance in crops.

Materials and methods

Plant materials and growth conditions

The rice (*Oryza sativa*) varieties Zhonghua11 (ZH11) and *Nipponbare* (NIP), the B73 wild-type maize were used in this study. The *osburp3* and *ossus1* mutant lines were purchased from the knockout mutant library of Biogle (Biogle Genome Editing Center). For the construction of OE-SLR1 and OE-OsBURP3 lines, the full coding sequences of SLR1 and OsBURP3 were cloned and inserted into the binary vector pCAMBIA1301, which were then transformed into NIP and ZH11 background by *Agrobacterium tumefaciens*.

Rice seeds were germinated for 3 days under 37 °C before transferred into Yoshida liquid medium (NSP1040; Coolaber, Beijing, China) and grown in a growth chamber at 28 °C with 16-h light/8-h dark cycles. For PEG6000 treatment, 12-day-old rice seedlings were treated with 20% PEG6000 for 7 days and then recovered for 3 days in Yoshida liquid medium (NSP1040; Coolaber) (*OsBURP3* overexpression lines, *OsSUS1* knock out lines and WT that corresponds to them were treated for 5 days). For soil drought tolerance assay, germinated seeds were sown in a cultivation box ($40 \times 30 \times 10\ cm^3$) filled with 1500 g of soil (vermiculite and substrate in a ratio of 1:1). After sowing for 12 days, the drought treatment was administered by withholding water until the leaf gradually rolled and withered. The plants were then rewatered and the surviving plants with green and healthy young leaves after rehydration were counted (Sun *et al.*, 2022; Xie *et al.*, 2023). At least three independent experiments, each involving a minimum of 24 plants per line, were used for statistically analysis of survival rates. For GA and PAC treatment experiments, 12-day-old seedlings were planted in Yoshida liquid medium (NSP1040; Coolaber) containing 100 μM GA3 (G7645; Sigma, St. Louis, MO, USA) or PAC (S18040; Shyuanye, Shanghai, China) for 3 days.

Scanning electron microscopy

For scanning electron microscopic analysis, 2-week-old seedlings were treated by withholding water for 5 days and cut into 3 mm^2 pieces, fixed with 2.5% glutaraldehyde and immediately placed under vacuum until the samples were completely submerged in the liquid. The samples were transferred into fresh 2.5% glutaraldehyde and incubated at 4 °C overnight, followed by successive washes with 30%, 50%, 70%, 80% and 90% ethanol for 10 min each, and finally with 100% ethanol twice for 10 min. The samples were subsequently critical-point dried, sputter coated with gold in an ion sputter (E-100, Japan) and examined under a JEM-1230 electron microscope.

RNA isolation and gene expression analysis

To analyse gene expression changes induced by drought stress, 2-week-old seedlings of ZH11 were dehydrated for 10 h and samples were collected every 2 h for five times. To analyse the gene expression changes under GA treatment, 2-week-old seedlings of ZH11 were treated with 100 μM GA for 32 h and samples were collected after 2, 4, 8, 16 and 32 h of treatment. The flag leaves of 4-week-old seedlings were used to analyse the gene expression in different transgenic lines.

Total RNA was extracted using a TRIzol reagent following the manufacturer's protocol (420810; Ambion, Austin, TX, USA). Complementary DNA was synthesized using HiScript Q RT SuperMix for quantitative PCR (R233-01; Vazyme, Nanjing, China). The quantitative RT-PCR analysis was performed using the Hieff qPCR SYBR Green Master Mix (11201ES03; Yeasen, Shanghai, China) in a Bio-Rad real-time instrument (CFX96). The data were analysed using the $2^{-\Delta\Delta C_t}$ method, with three biological and technical replicates.

Yeast two-hybrid assays

For Y2H screening, the full-length *SLR1* was cloned into the pGBKT7 vector as bait for matting with the rice cDNA library following the manufacturer's protocol (Clontech). 50 mM 3-aminotriazole (3-AT, a competitive inhibitor of HIS3 enzyme)

was applied to inhibit the strong self-transactivation activity of SLR1 in yeast. The positive colonies were grown in medium plates containing SD/-Trp/-Leu/-His/-Ade.

For Y2H assay, the All of the full-length CDS were cloned from rice and maize to confirm the interaction between the candidates in this study. The point-to-point validation was carried out as described previously (Hu *et al.*, 2012). All primers used in this study are listed in Table S4.

Bimolecular fluorescence complementation

To perform the BiFC assay, the CDS of *OsBURP3* and two truncated versions were cloned into the pSPYNE vector to construct OsBURP3-nYFP, OsBURP3$^{1\text{-}212}$-nYFP and OsBURP3$^{213\text{-}429}$-nYFP. The whole cDNA fragments of *SLR1* and *OsSUS1* were cloned into the pSPYCE vector to construct SLR1-cYFP and OsSUS1-cYFP, respectively. The constructs of OsBURP3-nYFP, SLR1-cYFP and OsSUS1-cYFP were co-transformed into rice protoplasts at 28 °C for 16–20 h in pairs. The YFP fluorescence signals were recorded using a confocal laser-scanning microscope (Leica TCS SP5). DAPI was used as a nuclear marker. More than 10 cells of positive signals were observed in each experiment.

Firefly luciferase complementation image assays

To further confirm the interaction between SLR1 with OsBURP3, and OsBURP3 with OsSUS1 in vivo. The transient expression experiments were performed in *N. benthamiana* leaves. The full-length CDS of *SLR1*, *OsBURP3* and *OsSUS1* were amplified and inserted into the 771-cLUC and 772-nLUC vectors to generate fusion constructs. Two constructs were transformed into the GV3101 strain containing the p19 silencing gene and then co-transformed into tobacco leaf epidermal cells via *Agrobacterium*-mediated infiltration. The injected leaves were sprayed with 1 mM luciferin (E1605; Promega, Madison, WI, USA), and the signals were captured using a Plant living imaging instrument (LB985; Berthold, Stuttgart, Germany) after 2 days incubation.

For the competitive assay, an equal amount of cLUC-OsBURP3 or nLUC-OsSUS1 was co-transformed with Ubi: SLR1 into tobacco leaf epidermal cells via *Agrobacterium*-mediated infiltration. The relative luciferase activity from three biological replicates was analysed with Image J software.

To investigate the interaction between DELLAs and BURPs, as well as between BURPs and SUSs in maize. The full-length CDS of DELLAs, BURPs and SUSs from maize were inserted into 771-cLUC and 772-nLUC vectors to generate fusion constructs. These corresponding vectors were then co-transformed into tobacco leaf epidermal cells, and the signals were captured.

Co-immunoprecipitation and IP-MS assay

For Co-IP assay, Actin-GFP, OsBURP3-GFP and SLR1-Flag vectors were separately transformed into *A. tumefaciens* strain GV3101 and co-expressed in *N. benthamiana* with indicated combinations. Total proteins were extracted using IP buffer [25 mM Tris–HCl, pH = 7.4, 150 mM NaCl, 1% NP-40, 5% Glycerol, 1 mM DTT and one protease inhibitor cocktail complete Mini tablet (Roche, Basel, Switzerland)] as described earlier, after which the lysates were incubated at 4 °C for 1 h, followed by centrifugation at 13 000 ***g*** for 30 min. The supernatants were incubated with 50 μL of anti-GFP magnetic beads (20564ES03; Yeasen) at 4 °C for 3 h for immunoprecipitation. The immunoprecipitates were collected for sodium dodecyl sulfate-polyacrylamide gel electrophoresis (SDS-PAGE) and detected with Anti-GFP (1:3000) and Anti-Flag (1:3000) antibodies (Chen *et al.*, 2021).

To identify the interaction proteins of OsBURP3, the IP-MS assay was performed. Total proteins were extracted from *OsBURP3* transgenic plants and WT plants with IP buffer, followed by incubation with Anti-Myc at 4 °C for 3 h. After washing three times with IP buffer, the immunoprecipitated protein mixture was analysed by LC–MS/MS using a Q Exactive HF-X system (Thermo Fisher Scientific, Waltham, MA, USA). The spectrum data were analysed using MASCOT.

Pull-down assay

To confirm the interactions between OsBURP3 with OsSUS1 in virto, the Pull-down assay was performed. The full-length CDS of *OsBURP3* was cloned into the pET28a-MBP vector, and the full-length CDS of *OsSUS1* was inserted into the pET28a vector to produce the recombinant proteins. The recombinant OsBURP3-MBP and OsSUS1-His were expressed in *E. coli* BL21 (DE3) and further purified for the pull-down assay. The OsBURP3-MBP and MBP recombinant proteins were incubated with MBP beads in a pull-down buffer [20 mM Tris–HCl (pH = 8.0), 200 mM NaCl, 0.5% Igepal CA-630, 1 mM EDTA (pH = 8.0) and one protease inhibitor cocktail complete Mini tablet (Roche)] at 4 °C for 3 h. Then, OsSUS1-His was added for an additional 2 h and subsequently washed five times, with the His tag protein used as a control. The supernatants were resolved using 10% SDS-PAGE and subjected to immunoblotting with Anti-His antibody (1:3000).

To examine the relationship among SLR1, OsBURP3 and OsSUS1, a competitive pull-down assay was conducted. The recombinant proteins SLR1-GST were expressed in *E. coli* BL21 (DE3) and purified with Glutathione Sepharose 4B beads. OsBURP3-MBP was first incubated with MBP beads in a pull-down buffer [20 mM Tris–HCl (pH = 8.0), 200 mM NaCl, 0.5% Igepal CA-630, 1 mM EDTA (pH = 8.0) and one protease inhibitor cocktail complete Mini tablet (Roche)] at 4 °C for 3 h. Then, OsSUS1-His and SLR1-GST were simultaneously added for an additional 2 h. The protein mixture was washed five times, resolved using 10% SDS-PAGE and subjected to immunoblotting with Anti-GST antibody (1:2000), Anti-MBP antibody (1:3000) and Anti-His antibody (1:3000).

In vivo and in vitro degradation assay

For the in vivo degradation assay of OsBURP3, the seedlings of OE-OsBURP3 lines were collected at 0, 2 and 4 h after treatment with 100 μM GA and 100 μM PAC, respectively. Total proteins were extracted with protein lysis buffer [25 mM Tris–HCl (pH = 7.4), 150 mM NaCl, 1% NP-40, 5% Glycerol, 1 mM DTT and one protease inhibitor cocktail complete Mini tablet (Roche)] and detected using 10% SDS-PAGE with Anti-SLR1 (1:1000), Anti-Myc (1:2000) and Anti-actin (1:10 000).

For the *in vitro* degradation assay of OsBURP3, the recombinant proteins of OsBURP3-MBP were expressed in *E. coli* BL21 and purified. Two-week-old seedlings of WT plants and *SLR1* over-expressing transgenic lines were harvested and ground into a fine powder with liquid nitrogen. Total proteins were subsequently extracted with lysis buffer [25 mM Tris–HCl (pH = 7.4), 150 mM NaCl, 1% NP-40, 5% glycerol and 1 mM DTT, and one protease inhibitor cocktail complete Mini tablet (Roche)] and adjusted to be at equal concentration with Pierce BCA protein assay kit (UD282965, Thermo Fisher Scientific). Equal amounts of protein supernatant were incubated with 200 ng OsBURP3-MBP for 0, 10, 20 and 30 min to estimate endogenous SLR1 and OsBURP3 protein levels, Anti-actin (1:10 000), and RbcL served as controls. Each experiment was repeated for more than three times.

Yeast three-hybrid assays

To verify the relationship among SLR1, OsBURP3 and OsSUS1, a Y3H assay was performed. The full-length CDS of *OsBURP3* was cloned into the pGADT7 vector, and the full-length CDSs of *SLR1* and *OsSUS1* were inserted into the MCSI and MCSII or MCSII and MCSI of pBridge vector, respectively. The pGADT7-OsBURP3 and pBridge-SLR1 (MCSI)-OsSUS1(MCSII) or pBridge-OsSUS1 (MCSI)-SLR1 (MCSII) were co-transformed into yeast in pairs and plated on SD/-Trp/-Met medium at 28 °C for 3 days. At least five colonies were diluted with 0.9% NaCl and transferred to SD-Trp/-Leu/-His/-Met medium plates.

Subcellular localization

To analyse the subcellular localization of OsBURP3, the full-length and truncated CDS of *OsBURP3* from ZH11 were cloned into the plant transient expression vector HBT95-sGFP. These constructs were then transformed into rice protoplasts followed by incubation in the dark for 16–20 h at 28 °C. The fluorescence signal was observed under a confocal laser-scanning microscope (Leica TCS SP5) with an excitation light of 488 nm for GFP and 405 nm for DAPI. More than 10 cells with strong positive signals were analysed In each experiment.

To detect the subcellular localization of OsSUS1, the full-length CDS of *OsSUS1* and *SLR1* from ZH11 were cloned into HBT95-sGFP and 1300 TB-mCherry vectors, respectively. The constructs were transformed into rice protoplasts and *N. benthamiana* leaves followed by treatment with a buffer containing 100 μM GA3 at 28 °C for 16–20 h. For drought treatment, the *N. benthamiana* leaves after complete transformation were treated with 200 mM mannitol for 4 and 8 h (Liu *et al.*, 2024). The fluorescence signal was observed under a confocal laser-scanning microscope (Leica TCS SP5). SLR1 was used as a nuclear marker and degraded by GA. At least 10 cells with positive signals were analysed in each experiment.

Enrichment and detection of nuclear and cytoplasm fractions

To quantify the enrichment of OsSUS1 in nucleus and cytoplasm fractions, the total, nucleus and cytosol were isolated. Two-week-old seedlings of WT (treated with 100 μM GA and 100 μM PAC) and transgenic lines of *OsBURP3* were harvested and ground into a fine powder with liquid nitrogen to detect the translocation of OsSUS1. The lysates were subsequently extracted with lysis buffer [20 mM Tris–HCl (pH 7.5), 20 mM KCl, 2 mM EDTA, 2.5 mM $MgCl_2$, 25% glycerol, 250 mM sucrose, 5 mM DTT and 0.4 mM PMSF]. The homogenate was filtered with a double layer of Miracloth (Calbiochem, Madison, WI, USA). The flow-through sample was considered as 'Total'. Next, the flow-through sample was centrifuged at 1000 ***g*** and 4 °C for 10 min. The supernatants were transferred to new tubes and then centrifuged again at 10 000 ***g*** and 4 °C for 10 min. This supernatant was collected as 'cytosol'. The pellet of the flow-through after centrifugation at 1000 ***g*** and 4 °C for 10 min was washed four times with 1 mL of nuclear resuspension buffer [20 mM Tris–HCl (pH 7.5), 25% glycerol, 2.5 mM $MgCl_2$, 0.3% Triton X-100 and 0.4 mM PMSF], followed by resuspension in 500 μL of NRB2 [20 mM Tris–HCl (pH 7.5), 0.25 M sucrose, 10 mM $MgCl_2$, 0.5% Triton X-100, 5 mM β-mercaptoethanol and 0.4 mM PMSF]. The resuspended nucleus was carefully overlaid on the top of NRB3 [20 mM Tris–HCl (pH 7.5), 1.7 M sucrose, 10 mM $MgCl_2$, 0.5% Triton X-100, 5 mM β-mercaptoethanol and 0.4 mM PMSF], and centrifuged at 1000 *g* in a swing-out rotor at 4 °C for 10 min. The pellet was collected as 'nucleus' (Fan *et al.*, 2023).

The fractions of total, nucleus and cytosol were adjusted to be at equal concentration with the BCA protein quantitative assay kit (UD282965, Thermo Fisher Scientific). The protein level of OsSUS1 was detected by Western blot using specific Anti-OsSUS1 (1:2000), Anti-Tubulin (1:3000) and Anti-histone H3 (1:3000) as controls.

Immunogold labeling analysis

For immunogold labeling analysis, leaves of 7-day-old *OsBURP3* transgenic, *SLR1* transgenic plants, and GA- or PAC-treated plants were cut into 0.1 mm pieces, fixed with 4% (v/v) glutaraldehyde in 0.1 M phosphate-buffered saline (PBS), pH 7.2 and stored at 4 °C overnight. The immunogold labeling signals were detected as described previously (Zhang *et al.*, 2022). The samples were washed three times with PBS for 30 min, and fixed with 2% (w/v) osmium tetroxide in PBS for 1 h at room temperature. Next, the samples were washed three times with MilliQ water, dehydrated (30% and 50% ethanol for 60 min; 70%, 80%, 85%, 90% and 95% ethanol for 30 min; 100% ethanol three times for 60 min) through a graded ethanol series and embedded in LR White resin for a couple of days. The sections (80–100 nm) were blocked and incubated with rabbit polyclonal antibody for OsSUS1 (ABclonal, custom made) under a dilution of 1/50 at 4 °C overnight. After washing three times with 1 × PBST, the samples were conjugated with particle-coupled secondary antibodies at a dilution of 1/50 (goat anti-rabbit IgG, 10 nm; Electron Microscopy Sciences), followed by observation using a transmission electron microscope (H7650, Hitachi, Tokyo, Japan) under a voltage of 80 kV.

Quantification of sucrose synthase activity, sucrose content and free proline content

To detect sucrose synthase activity, three-week-old seedlings of *OsSUS1* transgenic plants were collected and ground into a fine powder with liquid nitrogen, and the sucrose synthase activity was measured using a sucrose synthase activity assay kit (Boxbio, Beijing, China) according to the manufacturer's protocol. To detect the sucrose content, 2-week-old seedlings of rice and maize were collected at dusk after drought stress 5 days. These samples were then freeze-dried, ground and measured using a plant sucrose content assay kit (Boxbio) following the manufacturer's protocol.

To detect proline content, 12-day-old seedlings of different transgenic plants were treated with 20% PEG6000 for 6 h and the samples were freeze-dried, ground and measured using a plant sucrose content assay kit (Boxbio) following the manufacturer's protocol. Three biological replicates were used in every detection for above experiments.

Phylogenetic analysis

All the protein sequences of nine representatives of Gramineae crops were downloaded from the JGI/Phytozome database (https://phytozome-next.jgi.doe.gov/), and the HMM model (PF03181) of the BURP domain was downloaded from the Pfam database (http://pfam.xfam.org/). Then, the BURP families were identified in eight species using HMMsearch based on the HMM model of the BURP domain using E-value < 0.01. The phylogenetic tree was constructed using the neighbour-joining method of the MEGA11 software and visualized using the iTOL software (https://itol.embl.de/).

Acknowledgements

This work is supported by the National Natural Science Foundation of China (31871592), the Creative Research Groups of the Natural Science Foundation of Hubei Province (2020CFA009) and the Fundamental Research Funds for the Central Universities (2042022kf0015). We thank Professor Liangcai Peng from Huazhong Agricultural University for the gift of *OsSUS1* overexpression lines. Professor Limin Pi and Rongzhi Chen are also appreciated for their discussion and constructive suggestions. Dr. Wei Huang from Guangzhou biomedshine Co. Ltd is highly appreciated for his donation to this project.

Conflict of interest

The authors declare no competing interests.

Author contributions

J. Huang and J. Hu designed the experiment; J. Huang, B.X., F.X., Q.Y. and Y.R. performed most experiments; K.L. did the bioinformatics analysis; J. Huang., W.L., L.Z., Y.J., Y.T., L.P., Y.Z. and J. Hu analysed and discussed the results; J. Huang and J. Hu wrote the manuscript.

Accession numbers

Sequence from this article can be found in the GeneBank/EMBL databases under the following accession numbers: *SLR1*, LOC_Os03g49990; *OsBURP3*, LOC_Os01g53240; *OsSUS1*, LOC_Os03g28330; *Actin*, LOC_Os03g50885; *DWARF8*, Zm00001eb054480; *DWARF9*, Zm00001eb216610; *ZmBURP4*, Zm00001eb154060; *ZmBURP10*, Zm00001eb371370; *ZmSUS1*, Zm00001eb392880; *ZmSUS2*, Zm00001eb016290; *ZmSUS3*, Zm00001eb016250; *ZmSUS4*, Zm00001eb228780; *ZmSUS5*, Zm00001eb374090; *ZmSUS6*, Zm00001eb190590.

Data availability

The authors declare that all raw data supporting the findings of the study can be found within the paper and its Supporting Information. Source data are provided in this paper.

References

Achard, P., Baghour, M., Chapple, A., Hedden, P., Van Der Straeten, D., Genschik, P., Moritz, T. *et al.* (2007) The plant stress hormone ethylene controls floral transition via DELLA-dependent regulation of floral meristem-identity genes. *Proc. Natl Acad. Sci. USA*, **104**, 6484–6489.

Ahmad, H.M., Fiaz, S., Hafeez, S., Zahra, S., Shah, A.N., Gul, B., Aziz, O. *et al.* (2022) Plant growth-promoting rhizobacteria eliminate the effect of drought stress in plants: a review. *Front. Plant Sci.* **13**, 875774.

Anderson, R., Bayer, P.E. and Edwards, D. (2020) Climate change and the need for agricultural adaptation. *Curr. Opin. Plant Biol.* **56**, 197–202.

Bari, R. and Jones, J.D. (2009) Role of plant hormones in plant defence responses. *Plant Mol. Biol.* **69**, 473–488.

Chen, Y., Shen, J., Zhang, L., Qi, H., Yang, L., Wang, H., Wang, J. *et al.* (2021) Nuclear translocation of OsMFT1 that is impeded by OsFTIP1 promotes drought tolerance in rice. *Mol. Plant*, **14**, 1297–1311.

Chen, Q., Hu, T., Li, X., Song, C.P., Zhu, J.K., Chen, L. and Zhao, Y. (2022) Phosphorylation of SWEET sucrose transporters regulates plant root:shoot ratio under drought. *Nat. Plants*, **8**, 68–77.

Colebrook, E., Thomas, S., Phillips, A. and Hedden, P. (2014a) The role of gibberellin signalling in plant responses to abiotic stress. *J. Exp. Biol.* **217**, 67–75.

Cominelli, E., Conti, L., Tonelli, C. and Galbiati, M. (2013) Challenges and perspectives to improve crop drought and salinity tolerance. *New Biotechnol.* **30**, 355–361.

Cooper, M. and Messina, C. (2023) Breeding crops for drought-affected environments and improved climate resilience. *Plant Cell*, **35**, 162–186.

Davière, J. and Achard, P. (2016) A pivotal role of DELLAs in regulating multiple hormone signals. *Mol. Plant*, **9**, 10–20.

Dubois, M., Skirycz, A., Claeys, H., Maleux, K., Dhondt, S., De Bodt, S., Vanden Bossche, R. *et al.* (2013) Ethylene response factor6 acts as a central regulator of leaf growth under water-limiting conditions in Arabidopsis. *Plant Physiol.* **162**, 319–332.

Durand, M., Porcheron, B., Hennion, N., Maurousset, L., Lemoine, R. and Pourtau, N. (2016) Water deficit enhances C export to the roots in *Arabidopsis thaliana* plants with contribution of sucrose transporters in both shoot and roots. *Plant Physiol.* **170**, 1460–1479.

Fan, C., Wang, G., Wang, Y., Zhang, R., Wang, Y., Feng, S., Luo, K. *et al.* (2019) Sucrose synthase enhances hull size and grain weight by regulating cell division and starch accumulation in transgenic rice. *Int. J. Mol. Sci.* **20**(20), 4971.

Fan, B., Liao, K., Wang, L.-N., Shi, L.-L., Zhang, Y., Xu, L.-J., Zhou, Y. *et al.* (2023) Calcium-dependent activation of CPK12 facilitates its cytoplasm-to-nucleus translocation to potentiate plant hypoxia sensing by phosphorylating ERF-VII transcription factors. *Mol. Plant*, **16**, 979–998.

Fernando, A., Selvaraj, M., Ishitani, M., Nakashima, K., Shinozaki, K. and Yamaguchi-Shinozaki, K. (2021) How utilizing the genes involved in drought tolerance could tackle the climate change-related food crisis? *Mol. Plant*, **14**, 1601–1603.

Funfgeld, M., Wang, W., Ishihara, H., Arrivault, S., Feil, R., Smith, A.M., Stitt, M. *et al.* (2022) Sucrose synthases are not involved in starch synthesis in Arabidopsis leaves. *Nat. Plants*, **8**, 574–582.

Gupta, A., Rico-Medina, A. and Cano-Delgado, A.I. (2020) The physiology of plant responses to drought. *Science*, **368**, 266–269.

Han, C., Qiao, Y., Yao, L., Hao, W., Liu, Y., Shi, W., Fan, M. *et al.* (2022) TOR and SnRK1 fine tune SPEECHLESS transcription and protein stability to optimize stomatal development in response to exogenously supplied sugar. *New Phytol.* **234**, 107–121.

Harshavardhan, V.T., Van Son, L., Seiler, C., Junker, A., Weigelt-Fischer, K., Klukas, C., Altmann, T. *et al.* (2014) AtRD22 and AtUSPL1, members of the plant-specific BURP domain family involved in *Arabidopsis thaliana* drought tolerance. *PLoS One*, **9**, e110065.

Hedden, P. (2003) The genes of the green revolution. *Trends Genet.* **19**, 5–9.

Hu, J., Wang, K., Huang, W., Liu, G., Gao, Y., Wang, J., Huang, Q. *et al.* (2012) The rice pentatricopeptide repeat protein RF5 restores fertility in Hong-Lian cytoplasmic male-sterile lines via a complex with the glycine-rich protein GRP162. *Plant Cell*, **24**, 109–122.

Huang, X., Tian, H., Park, J., Oh, D.H., Hu, J., Zentella, R., Qiao, H. *et al.* (2023) The master growth regulator DELLA binding to histone H2A is essential for DELLA-mediated global transcription regulation. *Nat. Plants*, **9**, 1291–1305.

Juenger, T.E. and Verslues, P.E. (2023) Time for a drought experiment: do you know your plants' water status? *Plant Cell*, **35**, 10–23.

Kalladan, R., Lasky, J.R., Chang, T.Z., Sharma, S., Juenger, T.E. and Verslues, P.E. (2017) Natural variation identifies genes affecting drought-induced abscisic acid accumulation in *Arabidopsis thaliana*. *Proc. Natl Acad. Sci. USA*, **114**, 11536–11541.

Khan, Y., Xiong, Z., Zhang, H., Liu, S., Yaseen, T. and Hui, T. (2022) Expression and roles of GRAS gene family in plant growth, signal transduction, biotic and abiotic stress resistance and symbiosis formation-a review. *Plant Biol. (Stuttg.)* **24**, 404–416.

Kavi Kishor, P.B. and Sreenivasulu, N. (2013) Is proline accumulation per se correlated with stress tolerance or is proline homeostasis a more critical issue? *Plant Cell Environ.* **37**, 300–311.

Koch, K. (2004) Sucrose metabolism: regulatory mechanisms and pivotal roles in sugar sensing and plant development. *Curr. Opin. Plant Biol.* **7**, 235–246.

Li, K., Yu, R., Fan, L.M., Wei, N., Chen, H. and Deng, X.W. (2016) DELLA-mediated PIF degradation contributes to coordination of light and gibberellin signalling in Arabidopsis. *Nat. Commun.* **7**, 11868.

Liao, Z., Zhang, Y., Yu, Q., Fang, W., Chen, M., Li, T., Liu, Y. *et al*. (2023) Coordination of growth and drought responses by GA-ABA signaling in rice. *New Phytol.* **240**, 1149–1161.

Liu, Q., Wu, K., Harberd, N.P. and Fu, X. (2021) Green revolution DELLAs: from translational reinitiation to future sustainable agriculture. *Mol. Plant*, **14**, 547–549.

Liu, Z., Jiang, S., Jiang, L., Li, W., Tang, Y., He, W., Wang, M. *et al*. (2022) Transcription factor OsSGL is a regulator of starch synthesis and grain quality in rice. *J. Exp. Bot.* **73**, 3417–3430.

Liu, L., Zhang, L., Yang, L., Zheng, J., Jin, J., Tong, S. and Wu, Y. (2024) Genome-wide characterization and expression analysis of the HD-Zip II gene family in response to drought and GA3 stresses in *Nicotiana tabacum*. *Mol. Biol. Rep.* **51**, 581.

Magome, H., Yamaguchi, S., Hanada, A., Kamiya, Y. and Oda, K. (2008) The DDF1 transcriptional activator upregulates expression of a gibberellin-deactivating gene, GA2ox7, under high-salinity stress in Arabidopsis. *Plant J.* **56**, 613–626.

Mo, W., Tang, W., Du, Y., Jing, Y., Bu, Q. and Lin, R. (2020) PHYTOCHROME-INTERACTING FACTOR-LIKE14 and SLENDER RICE1 interaction controls seedling growth under salt stress. *Plant Physiol.* **184**, 506–517.

Murase, K., Hirano, Y., Sun, T.P. and Hakoshima, T. (2008) Gibberellin-induced DELLA recognition by the gibberellin receptor GID1. *Nature*, **456**, 459–463.

Nir, I., Shohat, H., Panizel, I., Olszewski, N., Aharoni, A. and Weiss, D. (2017) The tomato DELLA protein PROCERA acts in guard cells to promote stomatal closure. *Plant Cell*, **29**, 3186–3197.

Phokas, A. and Coates, J.C. (2021) Evolution of DELLA function and signaling in land plants. *Evol. Dev.* **23**, 137–154.

Saibo, N.J.M., Vriezen, W.H., Beemster, G.T.S. and Van Der Straeten, D. (2003) Growth and stomata development of Arabidopsis hypocotyls are controlled by gibberellins and modulated by ethylene and auxins. *Plant J.* **33**, 989–1000.

Sinclair, T.R. (2011) Challenges in breeding for yield increase for drought. *Trends Plant Sci.* **16**, 289–293.

Stein, O. and Granot, D. (2019) An overview of sucrose synthases in plants. *Front. Plant Sci.* **10**, 95.

Sun, X., Xiong, H., Jiang, C., Zhang, D., Yang, Z., Huang, Y., Zhu, W. *et al*. (2022) Natural variation of DROT1 confers drought adaptation in upland rice. *Nat. Commun.* **13**, 4265.

Tang, N., Ma, S., Zong, W., Yang, N., Lv, Y., Yan, C., Guo, Z. *et al*. (2016) MODD mediates deactivation and degradation of OsbZIP46 to negatively regulate ABA signaling and drought resistance in rice. *Plant Cell*, **28**, 2161–2177.

Uga, Y., Sugimoto, K., Ogawa, S., Rane, J., Ishitani, M., Hara, N., Kitomi, Y. *et al*. (2013) Control of root system architecture by DEEPER ROOTING 1 increases rice yield under drought conditions. *Nat. Genet.* **45**, 1097–1102.

Van De Velde, K., Ruelens, P., Geuten, K., Rohde, A. and Van Der Straeten, D. (2017) Exploiting DELLA signaling in cereals. *Trends Plant Sci.* **22**, 880–893.

Wang, H., Zhou, L., Fu, Y., Cheung, M.-Y., Wong, F.-L., Phang, T.-H., Sun, Z. *et al*. (2012) Expression of an apoplast-localized BURP-domain protein from soybean (GmRD22) enhances tolerance towards abiotic stress. *Plant Cell Environ.* **35**, 1932–1947.

Wang, H., Tang, J., Liu, J., Hu, J., Liu, J., Chen, Y., Cai, Z. *et al*. (2018) Abscisic acid signaling inhibits brassinosteroid signaling through dampening the dephosphorylation of BIN2 by ABI1 and ABI2. *Mol. Plant*, **11**, 315–325.

Xiao, N., Ma, H., Wang, W., Sun, Z., Li, P. and Xia, T. (2024) Overexpression of ZmSUS1 increased drought resistance of maize (*Zea mays* L.) by regulating sucrose metabolism and soluble sugar content. *Planta*, **259**, 43.

Xie, Z., Jin, L., Sun, Y., Zhan, C., Tang, S., Qin, T., Liu, N. *et al*. (2023) OsNAC120 balances plant growth and drought tolerance by integrating GA and ABA signaling in rice. *Plant Commun.* **53**, 100782.

Yang, D.L., Yao, J., Mei, C.S., Tong, X.H., Zeng, L.J., Li, Q., Xiao, L.T. *et al*. (2012) Plant hormone jasmonate prioritizes defense over growth by interfering with gibberellin signaling cascade. *Proc. Natl Acad. Sci. USA*, **109**, E1192–E1200.

Zhang, K., Wu, Z., Tang, D., Luo, K., Lu, H., Liu, Y., Dong, J. *et al*. (2017) Comparative transcriptome analysis reveals critical function of sucrose metabolism related-enzymes in starch accumulation in the storage root of sweet potato. *Front. Plant Sci.* **8**, 914.

Zhang, H., Zhou, J., Kan, Y., Shan, J., Ye, W., Dong, N., Guo, T. *et al*. (2022) A genetic module at one locus in rice protects chloroplasts to enhance thermotolerance. *Science*, **376**, 1293–1300.

Supporting information

Additional supporting information may be found online in the Supporting Information section at the end of the article.

Figure S1 Exogenous gibberellin (GA) treatment negatively regulates drought tolerance by degrading SLR1. [Correction added on 24 March 2025, after first online publication: Figure S1e is inserted in this version.]

Figure S2 The generation of SLENDER RICE 1 (*SLR1*) over-expressing lines and detection of its stomatal density and free proline under normal and drought stress.

Figure S3 Detection of self-transactivation activity of SLENDER RICE 1 (SLR1) and the interaction between SLR1 and OsBURP3 in yeast cells.

Figure S4 Phylogenetic analysis of homologous proteins.

Figure S5 Sequence alignment of OsBURP3 homologous proteins.

Figure S6 The action of SLENDER RICE 1 (SLR1) on the transcriptional level of OsBURP3.

Figure S7 The subcellular location of OsBURP3.

Figure S8 OsBURP3 negatively regulates drought tolerance in rice.

Figure S9 Agronomic traits examination of OsBURP3 transgenic lines.

Figure S10 The Y3H assay for the competition between SLENDER RICE 1 (SLR1) and OsSUS1.

Figure S11 GA signalling triggers nucleocytoplasmic translocation of OsSUS1.

Figure S12 OsBURP3 regulates the nucleocytoplasmic translocation of OsSUS1.

Figure S13 Immunogold labelling detection of OsSUS1.

Figure S14 Colocalization of OsSUS1 with different truncated of OsBURP3.

Figure S15 The expression pattern of OsSUS1.

Figure S16 The phenotype of OsSUS1 transgenic lines.

Figure S17 Sucrose-treated plants have increased survival rates under PEG6000 treatment.

Figure S18 Exogenous gibberellin (GA) treatment negatively regulates drought tolerance in maize.

Figure S19 Phylogenetic analysis of DELLA proteins and SUS proteins.

Figure S20 The interactions between DELLAs and ZmBURPs in maize.

Figure S21 The interactions between ZmBURPs and ZmSUSs in maize.

Table S1 Results of Y2H screen for OsBURP3.

Table S2 Phylogenetic analysis of homologous proteins of OsBURP3.

Table S3 Putative interacting proteins of OsBURP3 by IP-Mass assay.

Table S4 Primer used in this study.